

1 **Trans-ethnic and ancestry-specific blood-cell genetics in 746,667 individuals**
2 **from 5 global populations**

3
4 *A full list of authors and affiliations appears at the end of the paper.*

5
6 **Correspondence to:**

7 Paul L. Auer (pauer@uwm.edu)
8 Guillaume Lettre (guillaume.lettre@umontreal.ca)

9
10 *Summary: (148 words)*
11 *Main text: (2498 words)*
12 *4 figures, 1 table*

13 **SUMMARY** (148 words)

14 Most loci identified by GWAS have been found in populations of European ancestry (EA). In
15 trans-ethnic meta-analyses for 15 hematological traits in 746,667 participants, including 184,535
16 non-EA individuals, we identified 5,552 trait-variant associations at $P < 5 \times 10^{-9}$, including 71
17 novel loci not found in EA populations. We also identified novel ancestry-specific variants not
18 found in EA, including an *IL7* missense variant in South Asians associated with lymphocyte
19 count *in vivo* and *IL7* secretion levels *in vitro*. Fine-mapping prioritized variants annotated as
20 functional, and generated 95% credible sets that were 30% smaller when using the trans-ethnic
21 as opposed to the EA-only results. We explored the clinical significance and predictive value of
22 trans-ethnic variants in multiple populations, and compared genetic architecture and the impact
23 of natural selection on these blood phenotypes between populations. Altogether, our results for
24 hematological traits highlight the value of a more global representation of populations in genetic
25 studies.

26

27 INTRODUCTION

28 Blood-cell counts and indices are quantitative clinical laboratory measures that reflect
29 hematopoietic progenitor cell production, hemoglobin synthesis, maturation and release from the
30 bone marrow, and clearance of mature or senescent blood cells from the circulation. Quantitative
31 red blood cell (RBC), white blood cell (WBC) and platelet (PLT) traits exhibit strong heritability
32 ($h^2 \sim 30-80\%$)(Evans et al., 1999; Hinckley et al., 2013) and have been the subject of various
33 genome-wide association studies (GWAS), including a large study that identified >1000 genomic
34 loci in ~150,000 individuals of European-ancestry (EA)(Astle et al., 2016).

35

36 Importantly, the distribution of hematologic traits and prevalence of inherited hematologic
37 conditions differs by ethnicity. For example, the prevalence of anemia and microcytosis is higher
38 among African-ancestry (AFR) individuals compared to EA individuals in part due to the presence
39 of globin gene mutations (e.g. sickle cell, α/β -thalassemia) more common among African,
40 Mediterranean and Asian populations (Beutler and West, 2005; Raffield et al., 2018; Rana et al.,
41 1993). AFR individuals tend to have lower WBC and neutrophil counts partly because of the
42 Duffy/*DARC* null variant (Rappoport et al., 2019). Among Hispanics/Latinos (HA), a common
43 Native American functional intronic variant of *ACTN1* is associated with lower PLT count (Schick
44 et al., 2016).

45

46 Despite these observations, non-EA populations have been severely under-represented in most
47 blood-cell genetic studies to date (Popejoy and Fullerton, 2016; Popejoy et al., 2018; Wojcik et
48 al., 2019). Multiethnic GWAS have been recognized as more powerful for gene mapping due to
49 ancestry-specific differences in allele frequency, linkage disequilibrium (LD), and effect size of

50 causal variants (Li and Keating, 2014). Since blood cells play a key role in pathogen invasion,
51 defense and inflammatory responses, hematologic-associated genetic loci are particularly
52 predisposed to be differentiated across ancestral populations as a result of population history and
53 local evolutionary selective pressures (Ding et al., 2013; Lo et al., 2011; Raj et al., 2013). Given
54 the essential role of blood cells in tissue oxygen delivery, inflammatory responses, atherosclerosis,
55 and thrombosis (Byrnes and Wolberg, 2017; Chu et al., 2010; Colin et al., 2014; Tajuddin et al.,
56 2016), factors that contribute to such inter-population differences in blood-cell traits may also play
57 appreciable roles in the pathogenesis of chronic diseases and health disparities between
58 populations.
59

60 RESULTS

61 Trans-ethnic and ancestry-specific blood-cell traits genetic associations

62 We analyzed genotype-phenotype associations at up to 45 million autosomal variants in 746,667
63 participants, including 184,424 individuals of non-EA descent, for 15 traits (**Figure 1**,
64 **Supplementary Tables 1-4**, and **Methods**). The association results of the EA-specific meta-
65 analyses are reported separately in a companion paper. In the trans-ethnic meta-analyses, we
66 identified 5,552 trait-variant associations at $P < 5 \times 10^{-9}$, which include 71 novel associations not
67 reported in the EA-specific manuscript (**Supplementary Table 5**). Of the 5,552 trans-ethnic loci,
68 128 showed strong evidence of allelic effect heterogeneity across populations ($P_{\text{ancestry.hetero}} < 5 \times 10^{-9}$)
69 **(Supplementary Figure 1 and Supplementary Table 5)**. Ancestry-specific meta-analyses
70 revealed 28 novel trait-variant associations (**Figure 1 and Supplementary Tables 6-10**).
71 However, 19 out of these 21 novel AFR-specific associations map to chromosome 1 and are
72 associated with WBC or neutrophil counts, therefore reflecting long-range associations due to the
73 admixture signal at the Duffy/*DARC* locus (Reich et al., 2009). We attempted to replicate all novel
74 trans-ethnic or ancestry-specific genetic associations in the Million Veteran Program (MVP)
75 cohort (Gaziano et al., 2016). Of the 89 variant-trait associations that we could test in MVP, 86
76 had a consistent direction of effect (binomial $P = 6 \times 10^{-24}$), 72 had an association $P < 0.05$ (binomial
77 $P = 8 \times 10^{-79}$), and 44 met the Bonferroni-adjusted significance threshold of $P < 6 \times 10^{-4}$
78 **(Supplementary Table 11)**.

79

80 For 3,552 loci with evidence of a single association signal based on conditional analyses in EA
81 **(Supplementary Methods)**, we generated fine-mapping results for each trans-ethnic or ancestry-
82 specific dataset using an approximate Bayesian approach (**Methods**)(Wellcome Trust Case

83 Control et al., 2012). The 95% credible sets were smaller in the trans-ethnic meta-analyses than in
84 the EA or EAS meta-analyses (**Figure 2A**), indicating improved resolution owing to both
85 increased sample size and different LD patterns. When comparing loci discovered in both the trans
86 and EA analyses, we found that the 95% credible sets were 30% smaller among the trans results
87 (median (interquartile range) number of variants per 95% credible set was 4 (2-13) in trans vs. 5
88 (2-16) in EA, Wilcoxon's $P=3 \times 10^{-4}$). For instance, a locus on chromosome 9 associated with PLT
89 counts included seven variants in the EA 95% credible set but only one in the trans set, an increase
90 in fine-mapping resolution likely driven by limited LD at the locus in EAS (**Figure 2B**). In the
91 trans and EA results, respectively, we identified 433 and 403 loci with a single variant in the 95%
92 credible sets (**Figure 2C**).

93

94 Next, we assessed our fine-mapped 95% credible sets for the presence of functional variants, which
95 we defined as variants with coding consequences or those mapping to hematopoietic accessible
96 chromatin. Genomic annotation of the 95% credible sets of the trans, EA and EAS hematological
97 trait-associated loci revealed that the proportion of likely functional variants was higher among
98 those with high PPI (**Figure 2D**). The enrichment within high-PPI categories was particularly
99 notable for missense variants, but also observed for intronic and intergenic variants that map to
100 open chromatin regions in precursor or mature blood cells (**Figure 2D**)(Corces et al., 2016). We
101 used g-chromVAR to quantify the enrichment of trans, EA and EAS 95% credible set variants
102 within regions of accessible chromatin identified by ATAC-seq in 18 hematopoietic populations
103 (Corces et al., 2016; Ulirsch et al., 2019). We noted 22 significant trait-cell type enrichments using
104 the trans-ethnic credible sets, all of which were lineage specific, including RBC traits in erythroid
105 progenitors, platelet traits in megakaryocytes, and monocyte count in granulocyte-macrophage

106 progenitors (GMP) (**Figure 2E** and **Supplementary Table 12**). Cell-type enrichments were
107 largely consistent between fine-mapped traits found in the trans, EA and EAS loci. However, we
108 observed two noteworthy ancestry-specific differences: the EAS results revealed significant
109 enrichments in basophil count for the common myeloid progenitor (CMP) population and
110 eosinophil count for the GMP population, but neither pairing reached significance in the larger EA
111 meta-analyses (**Supplementary Figure 2**). These differences persisted even after controlling for
112 the number of loci tested in each ancestry. This is further supported by our finding that the genetic
113 correlations for these two traits between EA and EAS are the lowest among all studied blood
114 phenotypes (see below).

115

116 **Phenome-wide association studies (pheWAS)**

117 When we queried the 5,552 trans-ethnic genome-wide significant variants associated with blood-
118 cell traits in three distinct biobanks (EA individuals from UK Biobank (UKBB), Japanese from
119 Biobank Japan (BBJ), African Americans from BioVU (BioVU)), we identified 1,140 phenotype-
120 variant associations (**Supplementary Table 13**). These include 106 variants in BBJ, four variants
121 in BioVU, and 222 variants in the UKBB. Of the four variants significant in BioVU, three were
122 located at the β -globin locus and reflect the known clinical sequelae of sickle cell disease. Of the
123 1,140 associations, 246 were shared across at least two biobanks (**Methods**). Many of the
124 associations shared between BBJ and the UKBB were related to dyslipidemia and cardiovascular
125 diseases (**Supplementary Table 13**). Because of the large differences in sample sizes between the
126 three biobanks (**Methods**), we reasoned that lack of power was the likely explanation for why
127 associations were not shared across biobanks. However, it appears that differences in allele

128 frequencies across the three primary ancestries also played a role. Overall, unique associations had
129 greater differences in allele frequencies than shared associations (**Supplementary Figure 3**).

130

131 **Trans-ethnic predictions of hematological traits**

132 Polygenic trait scores (PTS) developed in a single ethnically homogeneous population tend to
133 underperform when tested in a different population (Grinde et al., 2019; Marquez-Luna et al.,
134 2017; Martin et al., 2019). We explored whether we could combine the genome-wide significant
135 trans-ethnic variants identified in our analyses into PTS that can predict blood-cell traits in a multi-
136 ethnic setting. First, we used trans-ethnic effect sizes as weights to compute PTS_{trans} for each trait,
137 and tested their performance in independent EA, AFR and HA participants from the BioMe
138 Biobank (**Methods**). As expected because our trans-ethnic meta-analyses are dominated by EA
139 individuals, PTS_{trans} were more predictive in EA, although their performance in HA was
140 comparable for several traits (lymphocyte and monocyte counts, mean PLT
141 volume)(**Supplementary Figure 4A** and **Supplementary Table 14**). Moreover, for neutrophil
142 and WBC counts, the variance explained by the PTS_{trans} was up to three times higher in AFR and
143 HA than in EA samples due to the inclusion of the strong Duffy/*DARC* locus (**Supplementary**
144 **Figure 4A**). Because these Duffy/*DARC* variants would not have been included in PTS derived
145 uniquely from EA association results, this illustrates an interesting feature of using trans-ethnic
146 variants for building polygenic predictors. Next, we asked if we could increase the variance
147 explained by calculating PTS using the same trans-ethnic variants but weighting them using
148 ancestry-specific as opposed to trans-ethnic effect sizes. PTS_{trans} outperformed ancestry-specific
149 PTS_{AFR} and PTS_{HA} in BioMe AFR and HA participants, respectively (**Supplementary Figure 4B-**
150 **C** and **Supplementary Table 14**). This result likely indicates that the discovery sample size for

151 these two populations is still too small to provide robust estimates of the true population-specific
152 effect sizes.

153

154 **Rare coding blood-cell-traits-associated variants**

155 The identification of rare coding variants has successfully pinpointed candidate genes for many
156 complex traits, including blood-cell phenotypes (Auer et al., 2014; Chami et al., 2016; Eicher et
157 al., 2016; Justice et al., 2019; Marouli et al., 2017; Mousas et al., 2017; Tajuddin et al., 2016). Our
158 trans-ethnic and non-EA ancestry-specific meta-analyses yielded 16 coding variants with minor
159 allele frequency (MAF) <1% (**Table 1** and **Supplementary Table 15**). This list includes variants
160 of clinical significance (variants in *TUBB1*, *GFI1B*, *HBB*, *MPL* and *SH2B3*) and variants that
161 nominate candidate genes within GWAS loci (*ABCA7*, *GMPR*) (**Table 1**). Our analyses also
162 retrieved a known missense variant in *EGLNI* (rs186996510) that is associated with high-altitude
163 adaptation and hemoglobin levels in Tibetans (Lorenzo et al., 2014; Xiang et al., 2013). We noted
164 a missense variant in *IL7* (rs201412253, Val18Ile) associated with increased lymphocyte count in
165 South Asians (SAS) ($P=4.4 \times 10^{-10}$) (**Figure 3A** and **Supplementary Table 16**). This variant is low-
166 frequency in SAS (MAF=2.6%) but rare in other populations (MAF <0.4%). *IL7* encodes
167 interleukin-7, a cytokine essential for B- and T-cell lymphopoiesis (Lin et al., 2017). *IL7* is
168 synthesized as a proprotein that is cleaved prior to secretion, and the *IL7*-Val18Ile variant localizes
169 to the *IL7* signal peptide comprising the first 25 amino acids. To determine if this variant alters
170 *IL7* secretion, we engineered HEK293 cells with either *IL7* allele (**Methods**). Although there was
171 no difference in *IL7* RNA expression levels (*t*-test $P=0.63$), we found that the *IL7*-18Ile allele,
172 which associates with higher lymphocyte counts in SAS individuals, significantly increased *IL7*
173 protein secretion in this heterologous cellular system (+83%, $P=2.7 \times 10^{-5}$) (**Figure 3B**).

174 Unfortunately, the relatively small sample size of the SAS cohort prevented us from testing
175 whether this *IL7* variant may be associated with other relevant phenotypes, such as cancer risk or
176 susceptibility to infections (Lin et al., 2017).

177

178 **Genetic architecture of blood-cell traits in EA and EAS populations**

179 We used several different approaches to quantify similarities and differences in genetic
180 architecture of hematologic traits across populations. Focusing on the two largest studied
181 populations, EA and EAS, we calculated heritability for all blood traits and found them to be highly
182 concordant between ancestries (Pearson's $r=0.75$, $P=0.0033$)(**Supplementary Table 17**)(Bulik-
183 Sullivan et al., 2015b). Likewise, within-ancestry genetic correlation coefficients (r_g) between
184 pairs of hematological traits were highly concordant across ancestries (Pearson's $r=0.97$,
185 $P<2.2\times 10^{-16}$)(**Supplementary Figure 5**)(Bulik-Sullivan et al., 2015a). We then used the Popcorn
186 method to directly measure genetic correlations for blood-cell traits between EA and EAS using
187 summary statistics for common variants (Brown et al., 2016). For all 13 traits available in both EA
188 and EAS, genetic correlations were high (lowest for basophils ($r_g=0.30$) and highest for MCH
189 ($r_g=0.66$)), but significantly different than 1 ($P<3\times 10^{-6}$)(**Supplementary Table 18**). This suggests
190 that even when considering only common variants, the genetic architecture of blood phenotypes is
191 substantially different between populations.

192

193 **Natural selection at blood-cell trait loci**

194 Natural selection can account for differences in association results between populations, as
195 highlighted by our analyses of rare coding variants which includes several loci known to be under
196 selection (*CD36*, *HBB*, *EGLNI*)(**Table 1**). To further explore this possibility, we assessed whether

197 variants that tag selective sweeps (tagSweeps, variants with the highest integrated haplotype score
198 (iHS)) within continental populations from the 1000 Genomes Project (1000G) are associated with
199 blood-cell phenotypes (Johnson and Voight, 2018). We found a genome-wide enrichment of
200 associations results between tagSweeps and hematological traits, particularly within EA, EAS and
201 AFR populations (**Supplementary Figure 6** and **Supplementary Table 19**). To rule out simple
202 overlaps due to the large number of sweeps and blood-cell trait loci, we compared the number of
203 genome-wide significant tagSweeps in EA, EAS and AFR with the number of significant variants
204 among 100 sets of matched variants (**Methods**). We found significant enrichment of selective
205 sweeps for WBC (EA, EAS, AFR), monocytes (EA, AFR), eosinophils (EA), neutrophils (AFR),
206 lymphocytes (EAS), and PLT (EA, EAS)(**Supplementary Table 20**).

207

208 In AFR and HA, the enrichments for WBC, neutrophils and monocytes were entirely driven by
209 selective sweeps on chromosome 1 near Duffy/*DARC* (Reich et al., 2009). Only three additional
210 loci shared evidence of associations with blood-cell traits and positive selection across
211 populations: HLA, *SH2B3* (Zhernakova et al., 2010) and *CYP3A5* (Chen et al., 2009). We found
212 eight and 100 non-overlapping selective sweeps with variants associated with hematological traits
213 in EAS and EA, respectively (**Supplementary Table 21**). Six of the eight EAS-specific tagSweeps
214 are also associated with blood-cell traits in EA participants, indicating that these regions do not
215 account for population differences in hematological trait regulation (**Supplementary Table 21**).
216 One of the remaining two variants is located at the *HBSIL-MYB* locus and, although it is not
217 associated with blood-cell traits in EA, there are many other variants near *MYB* associated with
218 blood phenotypes in EA (**Supplementary Table 6**). The remaining selective sweep highlighted
219 by this analysis is located upstream of *IL6* (**Figure 4**). The tagSweep at this locus, rs2188580, is

220 strongly associated with PLT count in EAS ($P_{EAS}=2.8 \times 10^{-9}$, $P_{EA}=0.0022$), is differentiated between
221 EAS and EA as indicated by the population branch statistic (PBS)(Yi et al., 2010)(C-allele
222 frequency in EAS=44%, 4% in EA; standardized $PBS_{EAS}=7.353$), and overlaps selective sweeps
223 identified in several EAS populations from the 1000G (e.g. $iHS_{CHS}=3.935$)(**Figure 4**). The *IL6*
224 locus has previously been associated with WBC traits in EA (Astle et al., 2016), but our finding is
225 the first report of its association with PLT. *IL6* encodes interleukin-6, a cytokine that is a
226 maturation factor for megakaryocytes, the precursors of PLT (Kimura et al., 1990). Further
227 supporting the role of IL6 signaling in PLT biology, a well-characterized missense variant in the
228 IL6 receptor gene (*IL6R*-rs2228145)(van Dongen et al., 2014) is also associated with PLT count
229 in EAS ($P=4.3 \times 10^{-6}$).

230

231 **DISCUSSION**

232 Our meta-analyses of 15 hematological traits in up to 746,667 individuals represents one of the
233 largest genetic study of clinically relevant complex human traits across diverse ancestral groups.
234 We have continued to expand the repertoire of loci and genes that contribute to interindividual
235 variation in blood-cell traits, with potential implications for hematological diseases, but also other
236 conditions such as cancer, immune and cardiovascular diseases. Our results hold a number of
237 implications for future human genetic studies. First, we showed that adding even a “modest”
238 number of non-EA participants to GWAS can yield important biology, such as the identification
239 of a lymphocyte count-associated *IL7* missense variants in 8,189 South Asians (**Figure 3**). Second,
240 loci that underlie variation in blood-cell traits represent a broad mixture of shared associations (i.e.
241 similar allele frequencies and effect sizes across populations) and heterogeneous associations (i.e.
242 dissimilar allele frequencies and effect sizes across populations). This result contributes to
243 mounting evidence that a full accounting of the genetic basis of complex human traits will require
244 a thorough catalog of global genetic and phenotypic variation. Third, because of heterogeneity
245 across populations in both allele frequencies and patterns of LD, fine-mapping of association
246 signals can be substantially aided by including multiple ancestries. This will have a dramatic
247 impact on the success of large-scale efforts aimed at functionally characterizing GWAS findings.
248 As more studies seek to unravel the causal variants that underlie complex traits associations, we
249 anticipate that genetic evidence from diverse ancestries will play an important role.

250

251 **SUPPLEMENTARY INFORMATION**

252 **Supplementary Information** is linked to the online version of the paper.

253

254 **ACKNOWLEDGMENTS**

255 We thank all participants, as well as Dr. John D. Rioux for providing the *IL7* ORF. A full list of
256 acknowledgments appears in the **Supplementary Information**. Part of this work was conducted
257 using the UK Biobank resource (Projects number 11707 and 13745).

258

259 **AUTHOR CONTRIBUTIONS**

260 *Writing Group (wrote and edited manuscript)*

261 Ming-Huei Chen, Laura M. Raffield, Abdou Mousas, Erik L. Bao, Alexander P. Reiner, Paul L.
262 Auer, Guillaume Lettre. All authors contributed and discussed the results, and commented on the
263 manuscript.

264

265 *Data preparation group (checked and prepared data from contributing cohorts for meta-analyses*
266 *and replication)*

267 Ming-Huei Chen, Laura M. Raffield, Abdou Mousas, Jennifer E. Huffman, Guillaume Lettre, Paul
268 L. Auer.

269

270 *Meta-analyses (discovery and replication)*

271 Ming-Huei Chen, Laura M. Raffield, Abdou Mousas, Saori Sakaue, Jennifer E. Huffman, Tao
272 Jiang, Parsa Akbari, Dragana Vuckovic, Erik L. Bao, Arden Moscati, Ken Sin Lo, Caleb A. Lareau,

273 Michael H. Guo, Tim Kacprowski, Fotis Koskeridis, Ani Manichaikul, Michael Preuss, Cassandra
274 N. Spracklen.

275

276 *Fine-mapping and functional annotation*

277 Abdou Mousas, Ming-Huei Chen, Laura M. Raffield, Erik L. Bao, Caleb A. Lareau, Ken Sin Lo,
278 Vijay G. Sankaran, Paul L. Auer, Guillaume Lettre.

279

280 *pheWAS, polygenic prediction, genetic architecture and natural selection*

281 Saori Sakaue, Arden Moscati, Regina Manansala, Minhui Chen, Ken Sin Lo, Huijun Qian, Yun
282 Li, Charleston W.K. Chiang, Ruth J.F. Loos, Alexander P. Reiner, Guillaume Lettre, Paul L. Auer.

283

284 *Functional characterization of IL7*

285 Mélissa Beaudoin, Véronique Laplante, Guillaume Lettre, Jean-François Gauchat

286

287 **AUTHOR INFORMATION**

288 Summary genetic association, fine-mapping and g-chromVAR results are available online:

289 <http://www.mhi-humangenetics.org/en/resources>. Competing financial interests are declared in the

290 **Supplementary Information**. Correspondence and requests should be addressed to P.L.A

291 (pauer@uwm.edu) or G.L. (guillaume.lettre@umontreal.ca).

292 **References**

- 293 Astle, W.J., Elding, H., Jiang, T., Allen, D., Ruklisa, D., Mann, A.L., Mead, D., Bouman, H.,
294 Riveros-Mckay, F., Kostadima, M.A., *et al.* (2016). The Allelic Landscape of Human Blood Cell
295 Trait Variation and Links to Common Complex Disease. *Cell* *167*, 1415-1429 e1419.
- 296 Auer, P.L., Johnsen, J.M., Johnson, A.D., Logsdon, B.A., Lange, L.A., Nalls, M.A., Zhang, G.,
297 Franceschini, N., Fox, K., Lange, E.M., *et al.* (2012). Imputation of exome sequence variants into
298 population- based samples and blood-cell-trait-associated loci in African Americans: NHLBI GO
299 Exome Sequencing Project. *Am J Hum Genet* *91*, 794-808.
- 300 Auer, P.L., Teumer, A., Schick, U., O'Shaughnessy, A., Lo, K.S., Chami, N., Carlson, C., de
301 Denus, S., Dube, M.P., Haessler, J., *et al.* (2014). Rare and low-frequency coding variants in
302 CXCR2 and other genes are associated with hematological traits. *Nat Genet*.
- 303 Beutler, E., and West, C. (2005). Hematologic differences between African-Americans and whites:
304 the roles of iron deficiency and alpha-thalassemia on hemoglobin levels and mean corpuscular
305 volume. *Blood* *106*, 740-745.
- 306 Brown, B.C., Asian Genetic Epidemiology Network Type 2 Diabetes, C., Ye, C.J., Price, A.L.,
307 and Zaitlen, N. (2016). Transethnic Genetic-Correlation Estimates from Summary Statistics. *Am*
308 *J Hum Genet* *99*, 76-88.
- 309 Bulik-Sullivan, B., Finucane, H.K., Anttila, V., Gusev, A., Day, F.R., Loh, P.R., ReproGen, C.,
310 Psychiatric Genomics, C., Genetic Consortium for Anorexia Nervosa of the Wellcome Trust Case
311 Control, C., Duncan, L., *et al.* (2015a). An atlas of genetic correlations across human diseases and
312 traits. *Nat Genet* *47*, 1236-1241.
- 313 Bulik-Sullivan, B.K., Loh, P.R., Finucane, H.K., Ripke, S., Yang, J., Schizophrenia Working
314 Group of the Psychiatric Genomics, C., Patterson, N., Daly, M.J., Price, A.L., and Neale, B.M.

315 (2015b). LD Score regression distinguishes confounding from polygenicity in genome-wide
316 association studies. *Nat Genet* 47, 291-295.

317 Bycroft, C., Freeman, C., Petkova, D., Band, G., Elliott, L.T., Sharp, K., Motyer, A., Vukcevic,
318 D., Delaneau, O., O'Connell, J., *et al.* (2018). The UK Biobank resource with deep phenotyping
319 and genomic data. *Nature* 562, 203-209.

320 Byrnes, J.R., and Wolberg, A.S. (2017). Red blood cells in thrombosis. *Blood* 130, 1795-1799.

321 Carroll, R.J., Bastarache, L., and Denny, J.C. (2014). R PheWAS: data analysis and plotting tools
322 for phenome-wide association studies in the R environment. *Bioinformatics* 30, 2375-2376.

323 Chami, N., Chen, M.H., Slater, A.J., Eicher, J.D., Evangelou, E., Tajuddin, S.M., Love-Gregory,
324 L., Kacprowski, T., Schick, U.M., Nomura, A., *et al.* (2016). Exome Genotyping Identifies
325 Pleiotropic Variants Associated with Red Blood Cell Traits. *Am J Hum Genet* 99, 8-21.

326 Chen, X., Wang, H., Zhou, G., Zhang, X., Dong, X., Zhi, L., Jin, L., and He, F. (2009). Molecular
327 population genetics of human CYP3A locus: signatures of positive selection and implications for
328 evolutionary environmental medicine. *Environ Health Perspect* 117, 1541-1548.

329 Chen, Y., Fang, F., Hu, Y., Liu, Q., Bu, D., Tan, M., Wu, L., and Zhu, P. (2016). The
330 Polymorphisms in LNK Gene Correlated to the Clinical Type of Myeloproliferative Neoplasms.
331 *PLoS One* 11, e0154183.

332 Chu, S.G., Becker, R.C., Berger, P.B., Bhatt, D.L., Eikelboom, J.W., Konkle, B., Mohler, E.R.,
333 Reilly, M.P., and Berger, J.S. (2010). Mean platelet volume as a predictor of cardiovascular risk:
334 a systematic review and meta-analysis. *J Thromb Haemost* 8, 148-156.

335 Colin, Y., Le Van Kim, C., and El Nemer, W. (2014). Red cell adhesion in human diseases. *Current*
336 *opinion in hematology* 21, 186-192.

337 Corces, M.R., Buenrostro, J.D., Wu, B., Greenside, P.G., Chan, S.M., Koenig, J.L., Snyder, M.P.,
338 Pritchard, J.K., Kundaje, A., Greenleaf, W.J., *et al.* (2016). Lineage-specific and single-cell
339 chromatin accessibility charts human hematopoiesis and leukemia evolution. *Nat Genet* 48, 1193-
340 1203.

341 Das, S., Forer, L., Schonherr, S., Sidore, C., Locke, A.E., Kwong, A., Vrieze, S.I., Chew, E.Y.,
342 Levy, S., McGue, M., *et al.* (2016). Next-generation genotype imputation service and methods.
343 *Nat Genet* 48, 1284-1287.

344 Delaneau, O., Zagury, J.F., and Marchini, J. (2013). Improved whole-chromosome phasing for
345 disease and population genetic studies. *Nat Methods* 10, 5-6.

346 Denny, J.C., Ritchie, M.D., Basford, M.A., Pulley, J.M., Bastarache, L., Brown-Gentry, K., Wang,
347 D., Masys, D.R., Roden, D.M., and Crawford, D.C. (2010). PheWAS: demonstrating the feasibility
348 of a phenome-wide scan to discover gene-disease associations. *Bioinformatics* 26, 1205-1210.

349 Ding, K., de Andrade, M., Manolio, T.A., Crawford, D.C., Rasmussen-Torvik, L.J., Ritchie, M.D.,
350 Denny, J.C., Masys, D.R., Jouni, H., Pachecho, J.A., *et al.* (2013). Genetic variants that confer
351 resistance to malaria are associated with red blood cell traits in African-Americans: an electronic
352 medical record-based genome-wide association study. *G3 (Bethesda)* 3, 1061-1068.

353 Eicher, J.D., Chami, N., Kacprowski, T., Nomura, A., Chen, M.H., Yanek, L.R., Tajuddin, S.M.,
354 Schick, U.M., Slater, A.J., Pankratz, N., *et al.* (2016). Platelet-Related Variants Identified by
355 Exomechip Meta-analysis in 157,293 Individuals. *Am J Hum Genet* 99, 40-55.

356 Evans, D.M., Frazer, I.H., and Martin, N.G. (1999). Genetic and environmental causes of variation
357 in basal levels of blood cells. *Twin Res* 2, 250-257.

358 Fang, H., Hui, Q., Lynch, J., Honerlaw, J., Assimes, T.L., Huang, J., Vujkovic, M., Damrauer,
359 S.M., Pyarajan, S., Gaziano, J.M., *et al.* (2019). Harmonizing Genetic Ancestry and Self-identified
360 Race/Ethnicity in Genome-wide Association Studies. *Am J Hum Genet* *105*, 763-772.

361 Gaziano, J.M., Concato, J., Brophy, M., Fiore, L., Pyarajan, S., Breeling, J., Whitbourne, S., Deen,
362 J., Shannon, C., Humphries, D., *et al.* (2016). Million Veteran Program: A mega-biobank to study
363 genetic influences on health and disease. *J Clin Epidemiol* *70*, 214-223.

364 Genomes Project, C., Abecasis, G.R., Auton, A., Brooks, L.D., DePristo, M.A., Durbin, R.M.,
365 Handsaker, R.E., Kang, H.M., Marth, G.T., and McVean, G.A. (2012). An integrated map of
366 genetic variation from 1,092 human genomes. *Nature* *491*, 56-65.

367 Grinde, K.E., Qi, Q., Thornton, T.A., Liu, S., Shadyab, A.H., Chan, K.H.K., Reiner, A.P., and
368 Sofer, T. (2019). Generalizing polygenic risk scores from Europeans to Hispanics/Latinos. *Genet*
369 *Epidemiol* *43*, 50-62.

370 Hinckley, J.D., Abbott, D., Burns, T.L., Heiman, M., Shapiro, A.D., Wang, K., and Di Paola, J.
371 (2013). Quantitative trait locus linkage analysis in a large Amish pedigree identifies novel
372 candidate loci for erythrocyte traits. *Mol Genet Genomic Med* *1*, 131-141.

373 Johnson, K.E., and Voight, B.F. (2018). Patterns of shared signatures of recent positive selection
374 across human populations. *Nat Ecol Evol* *2*, 713-720.

375 Justice, A.E., Karaderi, T., Highland, H.M., Young, K.L., Graff, M., Lu, Y., Turcot, V., Auer, P.L.,
376 Fine, R.S., Guo, X., *et al.* (2019). Protein-coding variants implicate novel genes related to lipid
377 homeostasis contributing to body-fat distribution. *Nat Genet* *51*, 452-469.

378 Kanai, M., Akiyama, M., Takahashi, A., Matoba, N., Momozawa, Y., Ikeda, M., Iwata, N.,
379 Ikegawa, S., Hirata, M., Matsuda, K., *et al.* (2018). Genetic analysis of quantitative traits in the
380 Japanese population links cell types to complex human diseases. *Nat Genet* *50*, 390-400.

381 Kang, H.M., Sul, J.H., Service, S.K., Zaitlen, N.A., Kong, S.Y., Freimer, N.B., Sabatti, C., and
382 Eskin, E. (2010). Variance component model to account for sample structure in genome-wide
383 association studies. *Nat Genet* 42, 348-354.

384 Kimura, H., Ishibashi, T., Uchida, T., Maruyama, Y., Friese, P., and Burstein, S.A. (1990).
385 Interleukin 6 is a differentiation factor for human megakaryocytes in vitro. *European journal of*
386 *immunology* 20, 1927-1931.

387 Klarin, D., Damrauer, S.M., Cho, K., Sun, Y.V., Teslovich, T.M., Honerlaw, J., Gagnon, D.R.,
388 DuVall, S.L., Li, J., Peloso, G.M., *et al.* (2018). Genetics of blood lipids among ~300,000 multi-
389 ethnic participants of the Million Veteran Program. *Nat Genet* 50, 1514-1523.

390 Kunishima, S., Kobayashi, R., Itoh, T.J., Hamaguchi, M., and Saito, H. (2009). Mutation of the
391 beta1-tubulin gene associated with congenital macrothrombocytopenia affecting microtubule
392 assembly. *Blood* 113, 458-461.

393 Li, Y.R., and Keating, B.J. (2014). Trans-ethnic genome-wide association studies: advantages and
394 challenges of mapping in diverse populations. *Genome Med* 6, 91.

395 Lin, J., Zhu, Z., Xiao, H., Wakefield, M.R., Ding, V.A., Bai, Q., and Fang, Y. (2017). The role of
396 IL-7 in Immunity and Cancer. *Anticancer Res* 37, 963-967.

397 Lo, K.S., Wilson, J.G., Lange, L.A., Folsom, A.R., Galarneau, G., Ganesh, S.K., Grant, S.F.,
398 Keating, B.J., McCarroll, S.A., Mohler, E.R., 3rd, *et al.* (2011). Genetic association analysis
399 highlights new loci that modulate hematological trait variation in Caucasians and African
400 Americans. *Hum Genet* 129, 307-317.

401 Loh, P.R., Kichaev, G., Gazal, S., Schoech, A.P., and Price, A.L. (2018). Mixed-model association
402 for biobank-scale datasets. *Nat Genet* 50, 906-908.

403 Loh, P.R., Palamara, P.F., and Price, A.L. (2016). Fast and accurate long-range phasing in a UK
404 Biobank cohort. *Nat Genet* 48, 811-816.

405 Lorenzo, F.R., Huff, C., Myllymaki, M., Olenchock, B., Swierczek, S., Tashi, T., Gordeuk, V.,
406 Wuren, T., Ri-Li, G., McClain, D.A., *et al.* (2014). A genetic mechanism for Tibetan high-altitude
407 adaptation. *Nat Genet* 46, 951-956.

408 Magi, R., Horikoshi, M., Sofer, T., Mahajan, A., Kitajima, H., Franceschini, N., McCarthy, M.I.,
409 Cogent-Kidney Consortium, T.D.G.C., and Morris, A.P. (2017). Trans-ethnic meta-regression of
410 genome-wide association studies accounting for ancestry increases power for discovery and
411 improves fine-mapping resolution. *Hum Mol Genet* 26, 3639-3650.

412 Magi, R., and Morris, A.P. (2010). GWAMA: software for genome-wide association meta-
413 analysis. *BMC Bioinformatics* 11, 288.

414 Mahajan, A., Taliun, D., Thurner, M., Robertson, N.R., Torres, J.M., Rayner, N.W., Payne, A.J.,
415 Steinthorsdottir, V., Scott, R.A., Grarup, N., *et al.* (2018). Fine-mapping type 2 diabetes loci to
416 single-variant resolution using high-density imputation and islet-specific epigenome maps. *Nat*
417 *Genet* 50, 1505-1513.

418 Marouli, E., Graff, M., Medina-Gomez, C., Lo, K.S., Wood, A.R., Kjaer, T.R., Fine, R.S., Lu, Y.,
419 Schurmann, C., Highland, H.M., *et al.* (2017). Rare and low-frequency coding variants alter human
420 adult height. *Nature* 542, 186-190.

421 Marquez-Luna, C., Loh, P.R., South Asian Type 2 Diabetes, C., Consortium, S.T.D., and Price,
422 A.L. (2017). Multiethnic polygenic risk scores improve risk prediction in diverse populations.
423 *Genet Epidemiol* 41, 811-823.

424 Martin, A.R., Kanai, M., Kamatani, Y., Okada, Y., Neale, B.M., and Daly, M.J. (2019). Clinical
425 use of current polygenic risk scores may exacerbate health disparities. *Nat Genet* 51, 584-591.

426 McCarthy, S., Das, S., Kretzschmar, W., Delaneau, O., Wood, A.R., Teumer, A., Kang, H.M.,
427 Fuchsberger, C., Danecek, P., Sharp, K., *et al.* (2016). A reference panel of 64,976 haplotypes for
428 genotype imputation. *Nat Genet* 48, 1279-1283.

429 Mousas, A., Ntritsos, G., Chen, M.H., Song, C., Huffman, J.E., Tzoulaki, I., Elliott, P., Psaty,
430 B.M., Blood-Cell, C., Auer, P.L., *et al.* (2017). Rare coding variants pinpoint genes that control
431 human hematological traits. *PLoS Genet* 13, e1006925.

432 Nagai, A., Hirata, M., Kamatani, Y., Muto, K., Matsuda, K., Kiyohara, Y., Ninomiya, T.,
433 Tamakoshi, A., Yamagata, Z., Mushiroda, T., *et al.* (2017). Overview of the BioBank Japan
434 Project: Study design and profile. *J Epidemiol* 27, S2-S8.

435 Pers, T.H., Timshel, P., and Hirschhorn, J.N. (2015). SNPsnap: a Web-based tool for identification
436 and annotation of matched SNPs. *Bioinformatics* 31, 418-420.

437 Popejoy, A.B., and Fullerton, S.M. (2016). Genomics is failing on diversity. *Nature* 538, 161-164.

438 Popejoy, A.B., Ritter, D.I., Crooks, K., Currey, E., Fullerton, S.M., Hindorff, L.A., Koenig, B.,
439 Ramos, E.M., Sorokin, E.P., Wand, H., *et al.* (2018). The clinical imperative for inclusivity: Race,
440 ethnicity, and ancestry (REA) in genomics. *Hum Mutat* 39, 1713-1720.

441 Rabbolini, D.J., Morel-Kopp, M.C., Chen, Q., Gabrielli, S., Dunlop, L.C., Chew, L.P., Blair, N.,
442 Brighton, T.A., Singh, N., Ng, A.P., *et al.* (2017). Thrombocytopenia and CD34 expression is
443 decoupled from alpha-granule deficiency with mutation of the first growth factor-independent 1B
444 zinc finger. *J Thromb Haemost* 15, 2245-2258.

445 Raffield, L.M., Ulirsch, J.C., Naik, R.P., Lessard, S., Handsaker, R.E., Jain, D., Kang, H.M.,
446 Pankratz, N., Auer, P.L., Bao, E.L., *et al.* (2018). Common alpha-globin variants modify
447 hematologic and other clinical phenotypes in sickle cell trait and disease. *PLoS Genet* 14,
448 e1007293.

449 Raj, T., Kuchroo, M., Replogle, J.M., Raychaudhuri, S., Stranger, B.E., and De Jager, P.L. (2013).
450 Common risk alleles for inflammatory diseases are targets of recent positive selection. *Am J Hum*
451 *Genet* 92, 517-529.

452 Rana, S.R., Sekhsaria, S., and Castro, O.L. (1993). Hemoglobin S and C traits: contributing causes
453 for decreased mean hematocrit in African-American children. *Pediatrics* 91, 800-802.

454 Rappoport, N., Simon, A.J., Amariglio, N., and Rechavi, G. (2019). The Duffy antigen receptor
455 for chemokines, ACKR1, - 'Jeanne DARC' of benign neutropenia. *Br J Haematol* 184, 497-507.

456 Reich, D., Nalls, M.A., Kao, W.H., Akyzbekova, E.L., Tandon, A., Patterson, N., Mullikin, J.,
457 Hsueh, W.C., Cheng, C.Y., Coresh, J., *et al.* (2009). Reduced neutrophil count in people of African
458 descent is due to a regulatory variant in the Duffy antigen receptor for chemokines gene. *PLoS*
459 *Genet* 5, e1000360.

460 Roden, D.M., Pulley, J.M., Basford, M.A., Bernard, G.R., Clayton, E.W., Balser, J.R., and Masys,
461 D.R. (2008). Development of a large-scale de-identified DNA biobank to enable personalized
462 medicine. *Clin Pharmacol Ther* 84, 362-369.

463 Schick, U.M., Jain, D., Hodonsky, C.J., Morrison, J.V., Davis, J.P., Brown, L., Sofer, T.,
464 Conomos, M.P., Schurmann, C., McHugh, C.P., *et al.* (2016). Genome-wide Association Study of
465 Platelet Count Identifies Ancestry-Specific Loci in Hispanic/Latino Americans. *Am J Hum Genet*
466 98, 229-242.

467 Tajuddin, S.M., Schick, U.M., Eicher, J.D., Chami, N., Giri, A., Brody, J.A., Hill, W.D.,
468 Kacprowski, T., Li, J., Lyytikainen, L.P., *et al.* (2016). Large-Scale Exome-wide Association
469 Analysis Identifies Loci for White Blood Cell Traits and Pleiotropy with Immune-Mediated
470 Diseases. *Am J Hum Genet* 99, 22-39.

471 Ulirsch, J.C., Lareau, C.A., Bao, E.L., Ludwig, L.S., Guo, M.H., Benner, C., Satpathy, A.T.,
472 Kartha, V.K., Salem, R.M., Hirschhorn, J.N., *et al.* (2019). Interrogation of human hematopoiesis
473 at single-cell and single-variant resolution. *Nat Genet* *51*, 683-693.

474 van Dongen, J., Jansen, R., Smit, D., Hottenga, J.J., Mbarek, H., Willemsen, G., Klufft, C.,
475 Collaborators, A., Penninx, B.W., Ferreira, M.A., *et al.* (2014). The contribution of the functional
476 IL6R polymorphism rs2228145, eQTLs and other genome-wide SNPs to the heritability of plasma
477 sIL-6R levels. *Behav Genet* *44*, 368-382.

478 Wakefield, J. (2007). A Bayesian measure of the probability of false discovery in genetic
479 epidemiology studies. *Am J Hum Genet* *81*, 208-227.

480 Wakefield, J. (2009). Bayes factors for genome-wide association studies: comparison with P-
481 values. *Genet Epidemiol* *33*, 79-86.

482 Weir, B.S., and Cockerham, C.C. (1984). Estimating F-Statistics for the Analysis of Population
483 Structure. *Evolution* *38*, 1358-1370.

484 Wellcome Trust Case Control, C., Maller, J.B., McVean, G., Byrnes, J., Vukcevic, D., Palin, K.,
485 Su, Z., Howson, J.M., Auton, A., Myers, S., *et al.* (2012). Bayesian refinement of association
486 signals for 14 loci in 3 common diseases. *Nat Genet* *44*, 1294-1301.

487 Willer, C.J., Li, Y., and Abecasis, G.R. (2010). METAL: Fast and efficient meta-analysis of
488 genomewide association scans. *Bioinformatics* *26*, 2190-2191.

489 Williams, A.L., Patterson, N., Glessner, J., Hakonarson, H., and Reich, D. (2012). Phasing of many
490 thousands of genotyped samples. *Am J Hum Genet* *91*, 238-251.

491 Winkler, T.W., Day, F.R., Croteau-Chonka, D.C., Wood, A.R., Locke, A.E., Magi, R., Ferreira,
492 T., Fall, T., Graff, M., Justice, A.E., *et al.* (2014). Quality control and conduct of genome-wide
493 association meta-analyses. *Nature protocols* *9*, 1192-1212.

494 Wojcik, G.L., Graff, M., Nishimura, K.K., Tao, R., Haessler, J., Gignoux, C.R., Highland, H.M.,
495 Patel, Y.M., Sorokin, E.P., Avery, C.L., *et al.* (2019). Genetic analyses of diverse populations
496 improves discovery for complex traits. *Nature* 570, 514-518.

497 Xiang, K., Ouzhuluobu, Peng, Y., Yang, Z., Zhang, X., Cui, C., Zhang, H., Li, M., Zhang, Y.,
498 Bianba, *et al.* (2013). Identification of a Tibetan-specific mutation in the hypoxic gene EGLN1
499 and its contribution to high-altitude adaptation. *Mol Biol Evol* 30, 1889-1898.

500 Yi, X., Liang, Y., Huerta-Sanchez, E., Jin, X., Cuo, Z.X., Pool, J.E., Xu, X., Jiang, H.,
501 Vinckenbosch, N., Korneliussen, T.S., *et al.* (2010). Sequencing of 50 human exomes reveals
502 adaptation to high altitude. *Science* 329, 75-78.

503 Zhernakova, A., Elbers, C.C., Ferwerda, B., Romanos, J., Trynka, G., Dubois, P.C., de Kovel,
504 C.G., Franke, L., Oosting, M., Barisani, D., *et al.* (2010). Evolutionary and functional analysis of
505 celiac risk loci reveals SH2B3 as a protective factor against bacterial infection. *Am J Hum Genet*
506 86, 970-977.

507 Zhou, W., Nielsen, J.B., Fritsche, L.G., Dey, R., Gabrielsen, M.E., Wolford, B.N., LeFaive, J.,
508 VandeHaar, P., Gagliano, S.A., Gifford, A., *et al.* (2018). Efficiently controlling for case-control
509 imbalance and sample relatedness in large-scale genetic association studies. *Nat Genet* 50, 1335-
510 1341.

511

512 **Figure legends**

513 **Figure 1.** Trans-ethnic and ancestry-specific meta-analyses of blood-cell traits. **(a)** Study design
514 of the project. We used a fixed-effect meta-analysis strategy to analyze genetic associations within
515 each of the five populations available, and a mega-regression approach that considers allele
516 frequency heterogeneity for the trans-ethnic association tests. **(b)** Most blood-cell trait-associated
517 loci physically overlap between populations. Despite different sample sizes between populations,
518 we note that few loci are found in a single population, suggesting shared genetic architecture.

519

520 **Figure 2.** Fine-mapping of loci associated with hematological traits highlights likely functional
521 variants. **(a)** We restricted fine-mapping to loci with evidence for a single association signal in
522 European-ancestry (EA) populations. There are no such loci in Hispanic Americans. The 95%
523 credible sets in the trans-ethnic meta-analyses are smaller than in the EA or East-Asian-ancestry
524 (EAS) meta-analyses. **(b)** Trans-ethnic fine-mapping of a platelet locus. In EA individuals, the
525 95% credible set include 7 variants with posterior probability of inclusion (PPI) >0.04 and strong
526 pairwise linkage disequilibrium (LD) with the sentinel variants rs10758481 ($r^2 > 0.93$ in GBR from
527 1000 Genomes Project, middle panel). LD is similarly strong in African-, Hispanic/South
528 American-, and South-Asian-ancestry populations from the 1000 Genomes Project. However, LD
529 is weaker in East Asians ($r^2 = 0.68$ in JPT from 1000 Genomes Project, bottom panel). In the trans-
530 ethnic meta-analysis, rs10758481 has a PPI >0.99 (top panel). In EA and EAS, LD is color-coded
531 based on pairwise r^2 with rs10758481. The dotted line indicates the genome-wide significance
532 threshold ($P < 5 \times 10^{-9}$). **(c)** Number of variants in 95% credible sets in each population analyzed. In
533 trans, EA and EAS, we identified 433, 403 and seven 95% credible sets with a single variant. **(d)**
534 Annotation of variants in trans, EA and EAS shows a similar pattern, with a larger proportion of

535 likely functional variants (e.g. missense, intergenic and intronic variants within ATAC-seq peaks)
536 among variants with higher posterior probability of inclusion (PPI). (e) g-chromVAR results for
537 trans variants within 95% credible sets for 15 traits. The Bonferroni-adjusted significance level
538 (corrected for 15 traits and 18 cell types) is indicated by the dotted line. mono, monocyte; gran,
539 granulocyte; ery, erythroid; mega, megakaryocyte; CD4, CD4+ T cell; CD8, CD8+ T cell; B, B
540 cell; NK, natural killer cell; mDC, myeloid dendritic cell; pDC, plasmacytoid dendritic cell; MPP,
541 multipotent progenitor; LMPP, lymphoid-primed multipotent progenitor; CMP, common myeloid
542 progenitor; CLP, common lymphoid progenitor; GMP, granulocyte–macrophage progenitor;
543 MEP, megakaryocyte–erythroid progenitor.

544

545 **Figure 3.** A South-Asian-ancestry *IL7* missense variant associates with increased lymphocyte
546 count in humans and *IL7* secretion in a heterologous cellular system. (a) Lymphocyte count
547 association results at the *IL7* locus in South Asians (SAS), European-ancestry participants (EA)
548 and East Asians (EAS). In SAS, there are 7 genome-wide significant variants near *IL7*, but only
549 rs201412253 is coding. Linkage disequilibrium (LD) r^2 is from 1000 Genomes Project SAS
550 populations. In EA, the sentinel variant is located downstream of *IL7*; rs201412253 is rare (minor
551 allele frequency= 4×10^{-4}) and not significant ($P=0.073$). In EAS, the locus is not associated with
552 lymphocyte count. rs201412253 is monomorphic in 1000 Genomes Project EA and EAS so we
553 could not calculate pairwise LD. (b) The 18Ile allele at *IL7*-rs201412253 increases *IL7* secretion
554 in a heterologous cellular system. Our ELISA assay did not detect secreted *IL7* in clones generated
555 with an empty vector. We tested eight independent clones for each *IL7* alleles. Each experiment
556 was done in duplicate, and we performed the experiments three times (grey circles). The black

557 dots and vertical lines indicate means and standard deviations. We assess statistical significance
558 by linear regression correcting for experimental batch effects.

559

560 **Figure 4.** Selective sweep and association with platelet count at the *IL6* locus in East Asians. The
561 grey rectangle highlights a genomic region upstream of *IL6* that is strongly associated with platelet
562 (PLT) count. This association signal is driven by results from East Asians (EAS), and is absent
563 from other populations, including European- (EA) and African-ancestry (AFR) individuals
564 (green). The region overlaps several selective sweeps detected in EAS from the 1000 Genomes
565 Project (CDX, CHS, JPT, KHV). In orange, we provide standardized population branch site
566 (stdPBS) metrics in EA and EAS, indicative of allele frequency differentiation at this locus
567 between these two populations.

568

569 **METHODS**

570 **Study design and participants**

571 All participants provided written informed consent and the project was approved by each
572 institution's ethical committee. **Supplementary Table 1** lists all participating cohorts. The SNPs
573 we identified are available from the NCBI dbSNP database of short genetic variations
574 (<https://www.ncbi.nlm.nih.gov/projects/SNP/>). No statistical methods were used to predetermine
575 sample size. The experiments were not randomized and the investigators were not blinded to
576 allocation during experiments and outcome assessment.

577

578 **Phenotypes**

579 Complete blood count (CBC) and related blood indices were analyzed as quantitative traits. The
580 descriptive statistics for each phenotype in each cohort analyzed are in **Supplementary Table 2**.
581 Exclusion criteria and phenotype modeling in the UK Biobank (UKBB)(European-ancestry
582 individuals), INTERVAL, and Biobank Japan (BBJ) have been described previously (Astle et al.,
583 2016; Kanai et al., 2018). For all other studies, we followed the protocol developed by the Blood-
584 Cell Consortium (Chami et al., 2016; Eicher et al., 2016; Tajuddin et al., 2016). Briefly, we
585 excluded when possible participants with blood cancer, acute medical/surgical illness,
586 myelodysplastic syndrome, bone marrow transplant, congenital/hereditary anemia, HIV, end-stage
587 kidney disease, splenectomy, and cirrhosis, as well as pregnant women and those undergoing
588 chemotherapy or erythropoietin treatment. We also excluded extreme blood-cell measures:
589 $WBC > 200 \times 10^9$ cells/L, $HGB > 20$ g/dL, $HCT > 60\%$, and $PLT > 1000 \times 10^9$ cells/L. For WBC
590 subtypes, we analyzed \log_{10} -transformed absolute counts obtained by multiplying relative counts
591 with total WBC count. For all phenotypes in all studies, we corrected the blood-cell phenotypes

592 for sex, age, age-squared, the 10 first genetic principal components, and other cohort-specific
593 covariates (e.g. recruitment center) using linear regression analysis. We applied rank-based inverse
594 normal transformation to the residuals from the regression analysis and used the normalized
595 residuals to test for association with genetic variants.

596

597 **Genotype quality-control and imputation**

598 The genotyping array and quality-control steps used by each cohort as well as their quality-control
599 steps are listed in **Supplementary Table 3**. Unless otherwise specified, all studies applied the
600 following criteria: samples were removed if the genotyping call rate was <95%, if they showed
601 excess heterozygosity, if we identified gender mismatches or sample duplicates, or if they appeared
602 as population outliers in principal component analyses nested with continental populations from
603 the 1000 Genomes Project (Genomes Project et al., 2012). We removed monomorphic variants, as
604 well as variants with Hardy-Weinberg $P < 1 \times 10^{-6}$ and call rate <98%.

605

606 Genotype imputation for the UKBB, INTERVAL, and BBJ have been described in details
607 elsewhere (Astle et al., 2016; Bycroft et al., 2018; Kanai et al., 2018). For all other studies, unless
608 specified in **Supplementary Table 3**, we applied the following steps for genotype imputation of
609 autosomal variants. We aligned all alleles on the forward strand of build 37/hg19 of the human
610 reference genome (<http://www.well.ox.ac.uk/~wrayner/strand>) and converted files into the VCF
611 format. We then applied checkVCF (<http://genome.sph.umich.edu/wiki/CheckVCF.py>) to confirm
612 strand and allele orientation. We carried out genotype imputation using the University of Michigan
613 (<https://imputationserver.sph.umich.edu>) or the Sanger Institute (<https://imputation.sanger.ac.uk/>)
614 imputation servers. We phased genotype data using SHAPEIT (Delaneau et al., 2013), EAGLE

615 (Loh et al., 2016), or HAPI-UR (Williams et al., 2012). For populations of European ancestry, we
616 used reference haplotypes from the Haplotype Reference Consortium (HRC r1.1 2016) for
617 imputation (McCarthy et al., 2016), whereas reference haplotypes from the 1000 Genomes Project
618 (Phase 3, Version 5)(Genomes Project et al., 2012) were used for non-European ancestry
619 participants.

620

621 **Study-level statistical analyses**

622 We tested an additive genetic model of association between genotype imputation doses and inverse
623 normal transformed blood-cell phenotypes. We analyzed the major ancestry groups (European
624 (EA), East Asian (EAS), African (AFR), Hispanic-Latino (HL), South Asian (SAS)) separately
625 and used linear mixed-effect models implemented in BOLT-LMM (Loh et al., 2018), EPACTS
626 (<https://genome.sph.umich.edu/wiki/EPACTS>), or EMMAX (Kang et al., 2010) to account for
627 cryptic and known relatedness. Autosomal single nucleotide variants were analyzed in all
628 contributing studies. For simplicity, we only analyzed insertion-deletion (indel) variants from
629 UKBB and INTERVAL, since a similar reference panel was used for genotype imputation.

630

631 **Centralized quality-control and meta-analyses**

632 We performed a centralized quality-control check on the association results of each single study
633 using EasyQC (v9.0)(Winkler et al., 2014). By mapping variants of each study to the appropriate
634 ethnicity reference panel (HRC for EA and 1000 Genomes Project Phase3 for non-EA
635 participants), we were able to harmonize alleles and markers across all studies. We were also able
636 to assess the presence of flipped alleles per study and check for excessive allele frequency
637 discrepancies using allele frequency reference data. We also inspected quantile-quantile (QQ)

638 plots generated by EasyQC and the corresponding genomic inflation factors as well as SE-N plots
639 (inverse of the median standard error vs. the square root of the sample size) to evaluate potential
640 issues with, for example, trait transformation or unaccounted relatedness. We removed variants
641 with imputation quality metric (INFO score) ≤ 0.4 . Except for three studies, we also removed
642 variants with minor allele count (MAC) ≤ 5 . For UKBB EA, Women Health Initiative (WHI), and
643 GERA (EA), we instead applied a MAC ≤ 20 filter because empirical observations suggested that
644 unusual inflation of the test statistics (i.e. extreme effect sizes and standard errors) was due to rarer
645 variants. To simplify handling of tri-allelic and indel variants, which have the same genomic
646 coordinates but different alleles, we created a unique variant ID for each tested variant.
647 Specifically, we assigned a chromosome:position(hg19)_allele1_allele2 unique ID to each variant,
648 in which the order of the allele in the ID was based on the lexicographical order or the indel length.
649 We performed inverse variance-weighted fixed-effect meta-analyses with GWAMA
650 (v2.2.2)(Magi and Morris, 2010) and trans-ethnic meta-analyses with MR-MEGA (v0.1.5)(Magi
651 et al., 2017). For MR-MEGA, we calculated four axes of genetic variation, the default
652 recommendation, to separate global population groups.

653

654 **Statistical significance, genomic inflation and locus definition**

655 For each meta-analysis, we calculated the genomic inflation factor (λ_{GC}) for all variants, which
656 were modest when considering the large sample sizes (λ_{GC} range: 0.9-1.2) (**Supplementary Table**
657 **4**). We used $\alpha \leq 5 \times 10^{-9}$ after GC-correction to declare statistical significance, accounting for the
658 inflation of the test statistics and the number of blood-cell traits analyzed. To count the number of
659 loci that we discovered, we first identified the most significant variants (with $P \leq 5 \times 10^{-9}$) and
660 extended the physical region around that variant 250-kb on each side. Overlapping loci were

661 merged, and we used the most significant variant within the interval as the sentinel variant. In this
662 manuscript, we defined as novel a locus if no variants were previously reported in the literature to
663 be associated with the specific blood-cell trait and if the locus is not reported in the companion
664 manuscript that focuses on EA-specific genetic discoveries.

665

666 **Million Veteran Program (MVP) blood-cell trait analyses for replication**

667 *Phenotyping.* Phenotyping methods published by the EMERGE Consortium and available on
668 PheKB (<https://phekb.org/>) were used for retrieving lab data and exclusion criteria for all blood
669 cell indices. This information was pulled from the VA electronic medical records for all MVP
670 participants. Lab data was subject to the Boston Lab Adjudication Protocol. This entails five steps:
671 (i) compile an initial spreadsheet of possible relevant lab tests, (ii) Subject Matter Expert (SME)
672 does an initial review of possible tests, (iii) analyst adds relevant LOINC codes for SME review,
673 (iv) second Subject Matter Expert (SME) review, (v) creation of a Lab Phenotype Table/Data Set.
674 After restricting to only outpatient labs and applying the EMERGE exclusion criteria, for each trait
675 and each person, the minimum, maximum, mean, median, SD, and number of labs was recorded.
676 Values were compared to those from UKBB (Astle et al., 2016).

677

678 *Genotyping.* DNA extracted from whole blood was genotyped using a customized Affymetrix
679 Axiom biobank array, the MVP 1.0 Genotyping Array. With 723,305 total DNA sequence variants,
680 the array is enriched for both common and rare variants of clinical importance in different ethnic
681 backgrounds (Klarin et al., 2018).

682

683 *Analysis.* The median lab value was the trait used for analysis. Linear regression models were run
684 under an additive model in plink2 on 1000G (v3p5) imputed dosages. Analyses were run using
685 models described above within each race/ethnicity stratum (AFR, ASN, EA, HA) classified based
686 on their genotype data using HARE (Fang et al., 2019). Meta-analyses for the trans-ethnic analyses
687 were completed in METAL (Willer et al., 2010).

688

689 **Heritabilities and genetic correlations**

690 We calculated heritabilities and genetic correlations between blood-cell traits within the EA and
691 EAS populations using default parameters implemented in the LD score regression method
692 (**Supplementary Table 17** and **Supplementary Figure 5**)(Bulik-Sullivan et al., 2015a; Bulik-
693 Sullivan et al., 2015b). For genetic correlation of the same phenotype between ancestral
694 populations, we used Popcorn (Brown et al., 2016). Briefly, Popcorn uses a Bayesian framework
695 to estimate, using genome-wide summary statistics, the genetic correlation of the same phenotype
696 but in two different populations (in our case, between EA and EAS). It reports the trans-ethnic
697 genetic-effect correlation (ρ_{ge}), i.e. the correlation coefficient of per-allele SNP effect sizes, but
698 also the trans-ethnic genetic impact correlation (ρ_{gi}), which includes a normalization of the effect
699 based on allele frequency (**Supplementary Table 18**). To address whether a difference in the
700 sample size for the EA and EAS meta-analyses could impact the Popcorn results, we repeated our
701 analyses using the current EAS results ($N_{max}=151,807$) and EA results from preliminary analyses
702 of the UKBB dataset ($N_{max}=87,265$)(Astle et al., 2016). These analyses confirmed that for common
703 variants, cross-ancestry EA-EAS genetic correlations are significantly different (but non-null).
704 Both LD score regression and Popcorn are not amenable to admixed populations, and cannot

705 handle rare variants. For these reasons, we limited these analyses to the large EA and EAS
706 populations and focused on common variants from the 1000 Genomes Project.

707

708 **Statistical fine-mapping**

709 No fine-mapping methods currently exist to handle admixed populations. Furthermore, for some
710 of the ethnic groups analyzed here, we did not have access to a sufficiently large reference panel
711 to properly account for LD, complicating conditional analyses and fine-mapping efforts. For these
712 reasons, we fine-mapped the ancestry-specific fixed-effect meta-analyses by adapting the method
713 proposed by Maller et al. (Wellcome Trust Case Control et al., 2012) in order to assign posterior
714 probability of inclusion (PPI) to each variant and construct 95% credible sets.

715

716 This method makes the strong assumption that there is a single independent causal variant at the
717 tested locus. For this reason, we limited our Bayesian fine-mapping to loci where we identified a
718 single independent association signal by conditional analysis in EA individuals from the UKBB
719 (**Supplementary Methods**). Because EA represented the largest group, we then inferred that there
720 was also a single association signal in the other populations at these loci, an inference that may not
721 always be right. Briefly, we added 250-kb on either side of genome-wide significant variants
722 ($P < 5 \times 10^{-9}$) and merged loci when they overlapped. For the loci identified in the ancestry-specific
723 meta-analyses, we converted P-values into approximate Bayes factors (aBF) using (Wakefield,
724 2009; Wellcome Trust Case Control et al., 2012):

725

726

$$aBF = \sqrt{\frac{SE^2}{SE^2 + \omega}} \exp \left[\frac{\omega \beta^2}{2SE^2(SE^2 + \omega)} \right]$$

727

728 where β and SE are the variant's effect size and standard error, respectively, and ω denotes the
729 prior variance in allelic effects, taken here to be 0.04 (Wakefield, 2007). For the trans-ethnic
730 results, we directly used Bayes factors calculated by MR-MEGA (Magi et al., 2017). We
731 calculated PPI of each variant by dividing the variant's aBF by the sum of the aBF for all the
732 variants within the locus. We generated the 95% credible sets by ordering all variants in a given
733 locus from the largest to the smallest PPI and by including variants until the cumulative sum of
734 the PPI $\geq 95\%$ (Mahajan et al., 2018). All variants that map to 95% credible sets are available
735 online (see **URL**).

736

737 **Functional annotation**

738 To derive basic functional annotation information, we annotated all variants included in 95%
739 credible sets from ancestry-specific and trans-ethnic meta-analyses with the Variant Effect
740 Predictor (VEP)(<https://useast.ensembl.org/info/docs/tools/vep/index.html>), compiling both all
741 consequences and the most severe consequence for Ensembl/GENCODE transcripts. We also
742 specifically annotated rare coding variants using VEP (defined as any variant with MAF $< 1\%$ in a
743 given analysis, with a GC-corrected P-value $< 5 \times 10^{-9}$, and annotated as a missense_variant,
744 stop_gained, stop_lost, splice_donor, or a splice_acceptor, regardless of fine-mapping
745 results). We removed all variants with a GC-corrected P-value $< 5 \times 10^{-9}$ in EA, in the MHC region,
746 and, in analyses including individuals with at least some African ancestry, on chromosome 1 for
747 neutrophils and total WBC count and for RBC traits near the chromosome 11 β -globin and the
748 chromosome 16 α -globin loci.

749

750 Bias-corrected enrichment of blood trait variants for chromatin accessibility of 18 hematopoietic
751 populations was performed using g-chromVAR, which has been previously described in detail
752 (Ulirsch et al., 2019). In brief, this method weights chromatin features by fine-mapped variant
753 posterior probabilities and computes the enrichment for each cell type versus an empirical
754 background matched for GC content and feature intensity. For chromatin feature input, we used a
755 consensus peak set for all hematopoietic cell types with a uniform width of 500 bp centered at the
756 summit. For variant input, we included all fine-mapped variants within 95% credible sets of the
757 trans-ethnic GWAS. We also ran g-chromVAR for each ancestry-specific meta-analysis, keeping
758 all other parameters the same, but using fine-mapped variants with the 95% credible sets of each
759 ancestry-specific study. Finally, to control for the number of loci tested within each ancestry-
760 specific study, we first ranked the loci of the largest cohort (i.e. EA) by sentinel variant p-value,
761 and then subset only the top n loci, where n equals the number of loci in the smaller cohort (e.g.
762 EAS) for the same trait. We then ran g-chromVAR on the subset of variants falling within these
763 top n loci.

764

765 **Phenome-wide association study (pheWAS) analysis**

766 *UK Biobank (UKBB)*. We extracted pheWAS results for a list of 5552 variants in UKBB ICD
767 PheWeb hosted at the University of Michigan (Accessed 21 August 2019). To account for severe
768 imbalance in case-control ratios, we selected the output from the SAIGE analyses
769 (<http://pheweb.sph.umich.edu/SAIGE-UKB/>) based on 408,961 samples from White British
770 participants (Zhou et al., 2018). In total, 1403 phecodes were tested for association. All results
771 were downloaded using R, and were parsed and organized into data table format using the
772 `data.table`, `rvest`, `stringr`, `dplyr` and `tidyr` packages.

773

774 *Biobank Japan (BBJ)*. We performed a pheWAS for the lead variants identified by the trans-ethnic
775 meta-analyses. From the list of all the significantly associated variants with blood cell-related
776 traits, we extracted those genotyped or imputed in the BBJ project ($n_{\text{SNP}} = 4,255$). Next, we curated
777 the phenotype record of the disease status and clinical values for the same individuals analyzed in
778 the discovery phase ($n_{\text{indiv}} = 143,988$). Then, we performed the logistic regression analyses for 22
779 binary traits (20 diseases and 2 behavioral habits) which had a sufficient number of case samples
780 ($n_{\text{case}} = 2,500$). Regression models were adjusted for age, sex and 20 principal components as
781 covariates. Trait-specific covariates are described elsewhere (Kanai et al., 2018).

782

783 *BioVU*. BioVU is the biobank of Vanderbilt University Medical Center (VUMC) that houses de-
784 identified DNA samples linked to phenotypic data derived from electronic health records (EHRs)
785 system of VUMC. The clinical information is updated every 1-3 months for the de-identified
786 EHRs. Detailed description of program operations, ethical considerations, and continuing
787 oversight and patient engagement have been published (Roden et al., 2008). DNA samples were
788 genotyped with genome-wide arrays including the Multi-Ethnic Global (MEGA) array, and the
789 genotype data were imputed into the HRC reference panel (McCarthy et al., 2016) using the
790 Michigan imputation server (Das et al., 2016). Imputed data and the 1000 Genome Project data
791 were combined to carry out principal component analysis (PCA) and African-American samples
792 were extracted for analysis based on the PCA plot. PheWAS were carried out for each SNP with
793 the specified allele (Denny et al., 2010). Phenotypes were derived from billing codes of EHRs as
794 described previously (Carroll et al., 2014). Each phenotype ('phecode') has defined case, control
795 and exclusion criteria. We required two codes on different visit days to instantiate a case for each

796 phecode. In total, 1815 phecodes were tested for association. Association between each binary
797 phecode and a SNP was assessed using logistic regression, while adjusting for covariates of age,
798 sex, genotyping array type/batch and 10 principal components of ancestry.

799

800 *Merging across biobanks.* We defined statistical significance within each biobank to be a
801 Bonferroni corrected level of $0.05/pq$, where p is the number of phecodes tested and q is the
802 number of variants tested. We merged results across UKBB and BioVU by matching on phecode,
803 as these two biobanks used the same phecode system for classifying outcomes. To merge with
804 BBJ, we cross-referenced the 22 outcomes in BBJ with the phecode library used by BioVU/UKBB.
805 Matches were determined based on phenotype similarity between the BioVU/UKBB phenotype
806 description and the outcomes described in Nagai *et al.* (Nagai *et al.*, 2017).

807

808 **Polygenic trait score (PTS) analyses**

809 We restricted these analyses to variant-trait associations that reached genome-wide significance
810 ($P < 5 \times 10^{-9}$) in the trans-ethnic MR-MEGA meta-analyses (**Supplementary Table 5**). For each of
811 these variant-trait pairs, we calculated an effect size – hereafter referred to as trans weights – using
812 the fixed-effect meta-analysis method implemented in GWAMA and all cohorts available (Magi
813 and Morris, 2010). For the same variants, we also retrieved the ancestry-specific effect sizes (or
814 weights). We calculated the PTS using plink2 by summing up the number of trait-increasing alleles
815 (or imputation doses) that were weighted by their corresponding trans (PTS_{trans}) or ancestry-
816 specific (PTS_{EA} , PTS_{AFR} , PTS_{HA}) weights. The variance explained by the PTS on corrected and
817 normalized blood-cell traits was calculated in R using linear regression. For these analyses, we

818 had access to 2,651 AFR, 5,048 EA and 4,281 HA BioMe participants, as well as 2546 AFR ARIC
819 participants, that were not used in the discovery effort.

820

821 **Analysis of natural selection**

822 To quantify the contribution of positive selection on blood-cell trait variation, we used the recent
823 map of selective sweeps identified in the different populations of the 1000 Genomes Project
824 (Johnson and Voight, 2018). We grouped the sweeps identified in the 26 1000 Genomes Project
825 populations into five larger populations that correspond to our ancestry-specific meta-analyses:
826 Europe-ancestry (CEU, TSI, GBR, FIN, IBS); East-Asian-ancestry (CHB, JPT, CHS, CDX,
827 KHV); African-ancestry (YRI, LWK, GWD, MSL, ESN, ASW, ACB); South-Asian-ancestry
828 (GIH, PJL, BEB, STU, ITU); and Hispanic/Latino-ancestry (MXL, PUR, CLM, PEL). Following
829 the nomenclature by Johnson and Voight(Johnson and Voight, 2018), each selective sweep is
830 summarized by the variant located within the sweep that has the highest iHS value. iHS (Integrated
831 Haplotype Score) is a statistic to quantify evidence of recent positive selection. A high positive
832 iHS score ($iHS > 2$) means that haplotypes on the ancestral allele background are longer compared
833 to derived allele background. A high negative iHS score ($iHS < -2$) means that the haplotypes on
834 the derived allele background are longer compared to the haplotypes associated with the ancestral
835 allele. We retrieved the blood-cell trait association results for these sweep-tagging SNPs from the
836 ancestry-specific meta-analyses (**Supplementary Table 19**). To determine if the inflation
837 observed in the QQ plots was significant, we generated 100 sets of SNPs that match the selective
838 sweep-tagging SNPs based on allele frequency, gene proximity, and the number of LD proxies in
839 European-ancestry, East-Asian-ancestry and African-ancestry individuals using SNPsnap (Pers et
840 al., 2015). For these analyses, we excluded the HLA region and variants in LD ($r^2 > 0.5$). We

841 computed empirical significance by tallying the number of sets with the same or more genome-
842 wide significant variants than the canonical sets of selective sweep-tagging SNPs (**Supplementary**
843 **Table 20**).

844

845 We also computed the population branch statistic (PBS)(Yi et al., 2010). PBS measures the amount
846 of allele frequency change in the population since its divergence from the other two populations.

847 For a target population, PBS is calculated as:

848

$$849 \quad PBS = \frac{T^{target,sister} + T^{target,outgroup} - T^{sister,outgroup}}{2}$$

850

851 where $T = -\log(1 - F_{ST})$ is an estimate of the divergence time between two populations. Here,
852 F_{ST} between each pair of populations was estimated using Weir and Cockerham's estimate (Weir
853 and Cockerham, 1984). We then divided all variants with calculated PBS into 50 bins of equal size
854 by derived allele count in the target population, and then standardized the raw PBS values within
855 each bin. To calculate PBS for Europe-ancestry (CEU, TSI, GBR, and IBS, without FIN), we used
856 YRI as an outgroup and East-Asian-ancestry (CHB, JPT, CHS, CDX, KHV) as a sister population;
857 for East-Asian-ancestry, we used YRI as an outgroup and Europe-ancestry as a sister population;
858 for YRI, we used East-Asian-ancestry as an outgroup and Europe-ancestry as a sister population.

859

860 **IL7 functional analyses**

861 We PCR amplified and cloned the *IL7* wildtype (rs201412253-Val18) and mutant (rs201412253-
862 18Ile) open reading frame (ORF) in the pcDNA5/FRT vector (ThermoFisher Scientific) using
863 HindIII and BamHI restriction sites (see **Supplementary Table 22** for ORF and primer

864 sequences). We validated the sequences of the two plasmids by Sanger Sequencing. Flip-In™-293
865 cells (ThermoFisher Scientific) at 80% confluency were transfected with 1:10 mixes of empty
866 pcDNA5 or pcDNA5 derivatives coding for IL7-Val8 or IL7-18Ile and pOG44 FLP recombinase
867 coding vector (ThermoFisher Scientific) using polyethylenimine. Transfectant clones were
868 expanded and selected in DMEM medium supplemented with 10% Foetal Bovine Serum, 4 mM
869 L-glutamine, 100 IU penicillin, 100 µg/ml streptomycin and 100 µg/ml hygromycin. We measured
870 the secretion of IL7 in eight independent clones for each *IL7* allele (rs201412253-Val18 and
871 rs201412253-18Ile) as well as in four clones generated with the empty vector by ELISA assay.
872 We used the High Sensitivity Quantikine HS ELISA kit from R & D Systems (Cat # HS750). We
873 seeded 100,000 cells per 12-wells plates and grew them for 6 days in DMEM glutamax plus 10%
874 FBS before doing the ELISA. We measured each supernatant in duplicate and seeded each of the
875 clones in triplicate. The whole experiment was done on three different weeks (three complete
876 biological replicates). We extracted total proteins from cells with RIPA buffer and we quantified
877 the lysates by BCA. We used this quantification to normalize the ELISA assays. We extracted total
878 RNA from ~500,000 cells using the Qiagen RNEasy kit (cat # 74136). We checked the quality of
879 the RNA by Bioanalyzer and quantified its concentration by Nanodrop. We reverse transcribed 1
880 µg of total RNA into cDNA using the ABI kit (Life Technologies Cat # 4368814). We used two
881 pairs of primers for *IL7* and assays for three normalizing genes (*HPRT*, *GAPDH*, *TBP*,
882 **Supplementary Table 22**). We followed the MIQE recommendations and performed the qPCR
883 reactions with the Sybergreen Platinum (Life Technologies Cat # 11733-046) on a Biorad CFX384
884 thermocycler.
885

886 **DATA AVAILABILITY STATEMENT**

887 All results are available at the following URL: <http://www.mhi-humangenetics.org/en/resources>

888

889 **URLs**

890 checkVCF: <http://genome.sph.umich.edu/wiki/CheckVCF.py>

891 EPACTS: <https://genome.sph.umich.edu/wiki/EPACTS>

892 Imputation servers: <https://imputationserver.sph.umich.edu> or <https://imputation.sanger.ac.uk/>

893 NCBI dbSNP: <https://www.ncbi.nlm.nih.gov/projects/SNP/>

894 PheKB: <https://phekb.org/>

895 Strand alignment resources: <http://www.well.ox.ac.uk/~wrayner/strand>

896 UK Biobank SAIGE results: <http://pheweb.sph.umich.edu/SAIGE-UKB/>

897 Variant Effect Predictor: <https://useast.ensembl.org/info/docs/tools/vep/index.html>

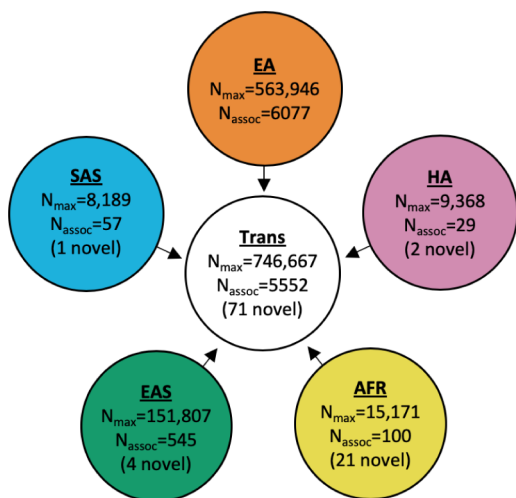
Table 1. Non-synonymous variants with a minor allele frequency (MAF) $\leq 1\%$ identified in non-European-ancestry (EA) populations or in the trans-ethnic meta-analyses. The population in which each variant was discovered is listed in the first column. Complete association results for each variant are available in **Supplementary Table 15**. Genomic coordinates (chr:position) are on build hg19. For the trans-ethnic results, mMAF corresponds to the mean MAF across all studies. EA, European-ancestry; EAS, East Asians; SAS, South Asians; AFR, African-ancestry; HA, Hispanics; PLT, platelet; NEU, neutrophil; MCH, mean corpuscular hemoglobin; MCV, mean corpuscular volume; MCHC, mean corpuscular hemoglobin concentration; MPV, mean platelet volume; EOS, eosinophil; MON, monocyte; RDW, red blood cell distribution width; LYM, lymphocyte; RBC, red blood cell count; HGB, hemoglobin; WBC, white blood cell.

Population	Position	Phenotype	rsID	mMAF (%)	P-value	Gene	Annotation	Note
EAS	1:43805737	PLT	rs117656396	0.9	5.20×10^{-12}	<i>MPL</i>	missense	Thrombopoietin receptor; MAF <0.1% in EA and SAS.
EAS	3:133476778	MCH	rs143019827	0.4	4.52×10^{-9}	<i>TF</i>	missense	Transferrin (iron binding protein); monomorphic in non-EAS populations.
EAS	3:184046450	PLT	rs112809828	0.08	2.03×10^{-35}	<i>EIF4G1</i>	missense	MAF <0.01% in EA. Located ~45kb from thrombopoietin (<i>THPO</i>).
EAS	6:16295278	MCH/MCV	rs78806162	0.4	$4.79 \times 10^{-14} / 4.82 \times 10^{-12}$	<i>GMPT</i>	missense	MAF <0.1% in SAS; monomorphic in EA.
EAS	6:41621210	MCH/MCV	rs201503063	1	$4.28 \times 10^{-9} / 1.03 \times 10^{-9}$	<i>MDFI</i>	missense	Monomorphic in non-EAS populations.
EAS	7:100014072	MCH/MCV	rs6957339	0.07	$3.65 \times 10^{-21} / 1.02 \times 10^{-10}$	<i>ZCWPW1</i>	missense	MAF in EA <0.03%; more common in AFR and HA populations (MAF=0.2-0.6%). Located ~204kb from <i>TFR2</i> .
EAS	19:1049396	LYM/WBC	rs201347186	0.6	$8.78 \times 10^{-13} / 6.53 \times 10^{-22}$	<i>ABCA7</i>	missense	Previous GWAS identified common missense SNPs in <i>ABCA7</i> associated with NEU (Astle et al., 2016); monomorphic in non-EAS populations.
EAS	20:57599434	PLT	rs121918555	0.06	1.27×10^{-13}	<i>TUBB1</i>	missense	Mutation previously characterized in Japanese patients with congenital macrothrombocytopenia (Kunishima et al., 2009); monomorphic in non-EAS populations.
SAS	9:135863848	MPV/PLT	rs527297896	0.5	$2.24 \times 10^{-19} / 3.57 \times 10^{-18}$	<i>GFIIB</i>	missense	Mutation previously identified in patients with thrombocytopenia without α -granule or bleeding defect (Rabbolini et al., 2017); monomorphic in non-SAS populations.
Trans	1:43803807	PLT	rs17292650	0.2	2.87×10^{-16}	<i>MPL</i>	missense	Thrombopoietin receptor; known common variant in AFR populations (MAF=4.2%)(Auer et al., 2012).
Trans	1:231557623	HCT	rs186996510	1	4.90×10^{-15}	<i>EGLN1</i>	missense	Low-frequency variant in EAS (MAF=4.1%) and AFR (3.2%), rare in SAS (0.6%) and EA (<0.01%). Associated with adaptation to

								hypoxia and HGB in Tibetans (Xiang et al., 2013).
Trans	7:80300449	RDW	rs3211938	0.3	5.75×10^{-14}	<i>CD36</i>	nonsense	Known common variant in AFR populations (MAF=9.3%)(Chami et al., 2016).
Trans	9:136083640	RBC	rs12336956	0.8	1.01×10^{-9}	<i>OBP2B</i>	missense	Association signal in EA (MAF=0.3%); MAF=3% in HL; MAF=19% in AFR. Located ~47kb from <i>ABO</i> .
Trans	11:5248232	LYM	rs334	0.2	9.50×10^{-16}	<i>HBB</i>	missense	Sickle cell anemia mutation, well known for RBC trait associations.
Trans	12:111856673	PLT	rs78894077	0.9	7.63×10^{-38}	<i>SH2B3</i>	missense	Common variant in EAS (MAF=3.6%). Associated with myeloproliferative neoplasms (Chen et al., 2016).
Trans	17:38062390	WBC	rs35266519	0.8	6.69×10^{-12}	<i>GSDMB</i>	missense	Rare across all populations. Previously reported for NEU count (Mousas et al., 2017).

FIGURE 1

a



b

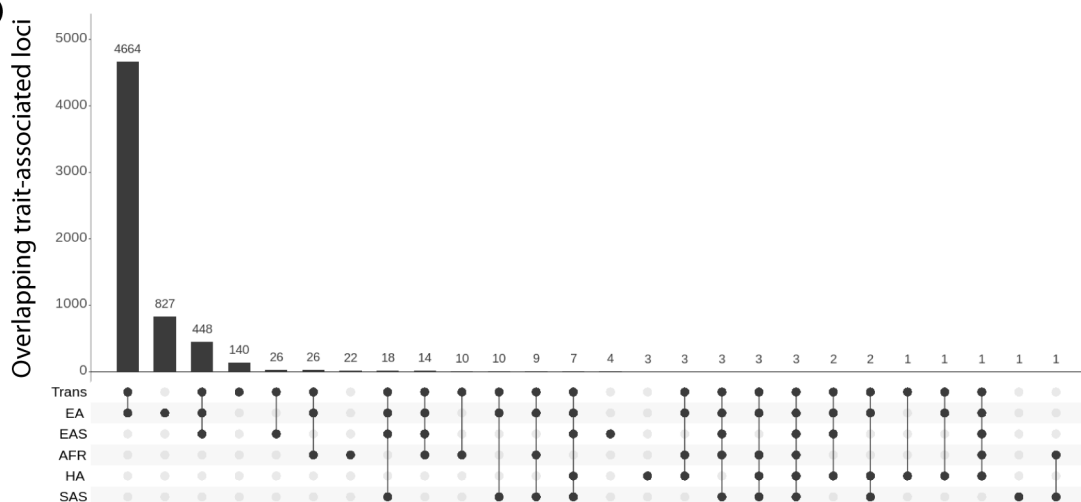


FIGURE 2

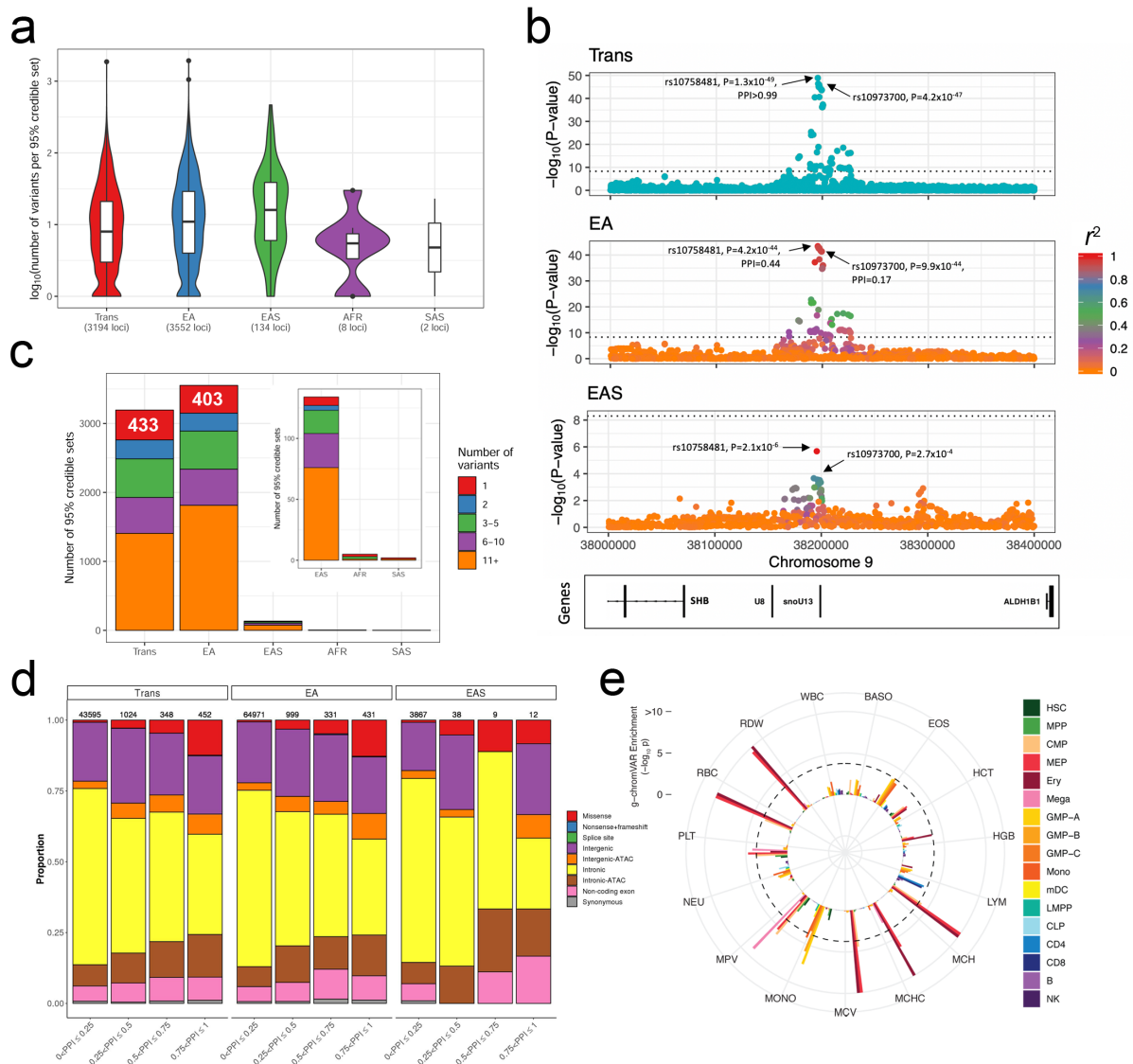


FIGURE 3

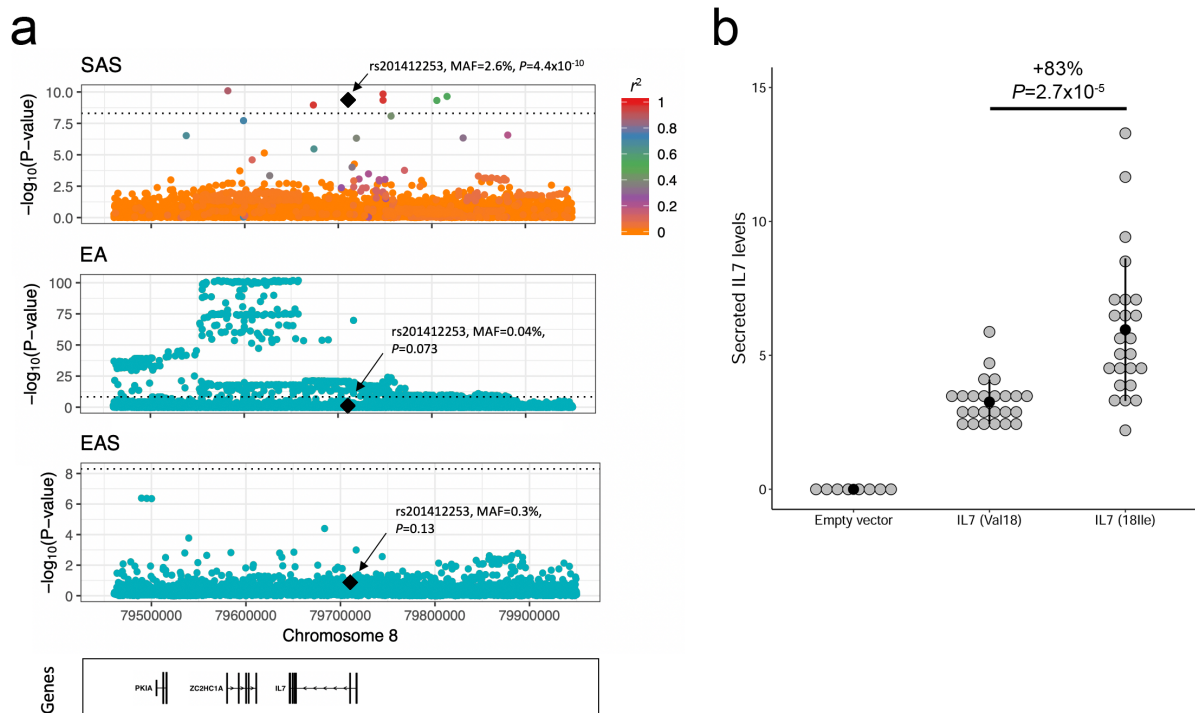
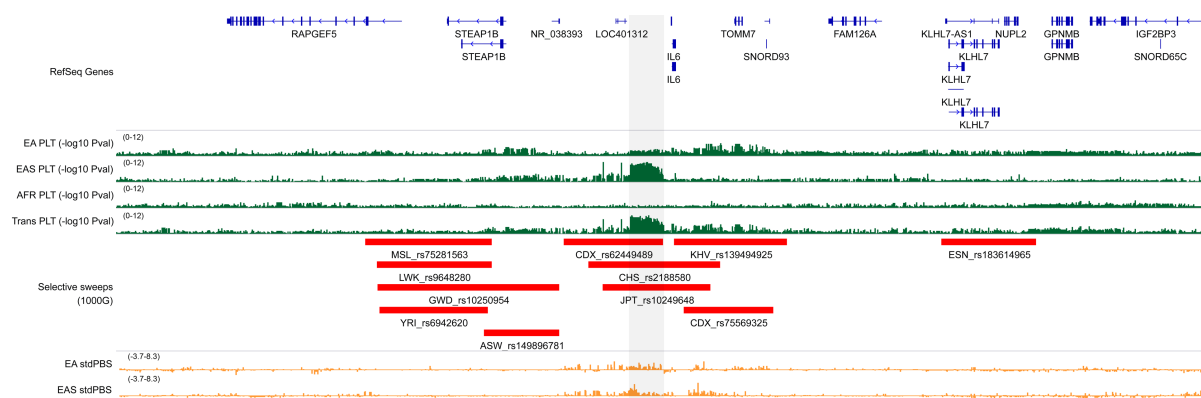


FIGURE 4



AUTHORLIST

Ming-Huei Chen^{1,2,*}, Laura M. Raffield^{3,*}, Abdou Mousas^{4,*}, Saori Sakaue^{5,6}, Jennifer E. Huffman⁷, Tao Jiang⁸, Parsa Akbari^{9,10,11}, Dragana Vuckovic^{11,12}, Erik L. Bao^{13,14}, Arden Moscati¹⁵, Xue Zhong¹⁶, Regina Manansala¹⁷, Véronique Laplante¹⁸, Minhui Chen¹⁹, Ken Sin Lo⁴, Huijun Qian²⁰, Caleb A. Lareau^{13,14}, Mélissa Beaudoin⁴, Masato Akiyama^{6,21}, Traci M. Bartz²², Yoav Ben-Shlomo²³, Andrew Beswick²⁴, Jette Bork-Jensen²⁵, Erwin P. Bottinger^{15,26}, Jennifer A. Brody²⁷, Frank J.A. van Rooij²⁸, Kumaraswamy Chitrala²⁹, Kelly Cho^{30,31,32}, Hélène Choquet³³, Adolfo Correa³⁴, John Danesh^{8,35,36,37,38,39}, Emanuele Di Angelantonio^{8,35,36,39}, Niki Dimou^{40,41}, Jingzhong Ding⁴², Paul Elliott^{43,44,45,46,47}, Tõnu Esko¹⁴, Michele K. Evans²⁹, James S. Floyd^{27,48}, Linda Broer⁴⁹, Niels Grarup²⁵, Michael H. Guo^{14,50}, Andreas Greinacher⁵¹, Jeff Haessler⁵², Torben Hansen²⁵, Joanna M. M. Howson⁸, Wei Huang⁵³, Eric Jorgenson³³, Tim Kacprowski^{54,55,56}, Mika Kähönen^{57,58}, Yoichiro Kamatani^{6,59}, Masahiro Kanai^{6,60}, Savita Karthikeyan⁸, Fotis Koskeridis⁴¹, Leslie A. Lange⁶¹, Terho Lehtimäki^{62,63}, Markus M. Lerch⁶⁴, Allan Linneberg^{65,66}, Yongmei Liu⁶⁷, Leo-Pekka Lyytikäinen^{62,63}, Ani Manichaikul⁶⁸, Koichi Matsuda⁶⁹, Karen L. Mohlke³, Nina Mononen^{62,63}, Yoshinori Murakami⁷⁰, Girish N. Nadkarni¹⁵, Matthias Nauck^{56,71}, Kjell Nikus^{72,73}, Willem H. Ouwehand^{11,36,39,74,75}, Nathan Pankratz⁷⁶, Oluf Pedersen²⁵, Michael Preuss¹⁵, Bruce M. Psaty^{27,77,78,79}, Olli T. Raitakari^{80,81,82}, David J. Roberts^{83,84}, Stephen S. Rich⁶⁸, Benjamin A.T. Rodriguez^{1,2}, Jonathan D. Rosen⁸⁵, Jerome I. Rotter⁸⁶, Petra Schubert³⁰, Cassandra N. Spracklen³, Praveen Surendran⁹, Hua Tang⁸⁷, Jean-Claude Tardif^{4,88}, Mohsen Ghanbari²⁸, Uwe Völker^{54,56}, Henry Völzke^{56,89}, Nicholas A. Watkins⁷⁵, Alan B. Zonderman²⁹, VA Million Veteran Program[†], Peter W.F. Wilson⁹⁰, Yun Li^{3,85,91}, Adam S. Butterworth^{8,35,36}, Jean-François Gauchat¹⁸, Charleston W.K. Chiang^{19,92}, Bingshan Li⁹³, Ruth J.F. Loos¹⁵, William J. Astle^{10,12,94}, Evangelos Evangelou^{41,43}, Vijay G. Sankaran^{13,14}, Yukinori Okada^{5,95}, Nicole Soranzo^{11,74}, Andrew D. Johnson^{1,2,§}, Alexander P. Reiner^{48,§}, Paul L. Auer^{17,§}, Guillaume Lettre^{4,88,§}

¹The Framingham Heart Study, National Heart, Lung and Blood Institute, Framingham, MA, USA, ²Population Sciences Branch, Division of Intramural Research, National Heart, Lung and Blood Institute, Framingham, MA, USA, ³Department of Genetics, University of North Carolina, Chapel Hill, NC, USA, ⁴Montreal Heart Institute, Montreal, Quebec, Canada, ⁵Department of Statistical Genetics, Osaka University Graduate School of Medicine, Suita, Osaka, Japan, ⁶Laboratory for Statistical Analysis, RIKEN Center for Integrative Medical Sciences, Yokohama, Kanagawa, Japan, ⁷Center for Population Genomics, Massachusetts Veterans Epidemiology Research and Information Center (MAVERIC), VA Boston Healthcare System, Boston, MA, USA, ⁸Department of Public Health and Primary Care, University of Cambridge, Cambridge, UK, ⁹MRC/BHF Cardiovascular Epidemiology Unit, Department of Public Health and Primary Care, University of Cambridge, Cambridge, UK, ¹⁰MRC Biostatistics Unit, University of Cambridge, Cambridge, UK, ¹¹Human Genetics, Wellcome Sanger Institute, Hinxton, UK, ¹²NIHR Blood and Transplant Research Unit in Donor Health and Genomics, Strangeways Laboratory, Cambridge, UK, ¹³Division of Hematology/Oncology, Boston Children's Hospital, Boston, MA, USA, ¹⁴Broad Institute of Harvard and MIT, Cambridge, MA, USA, ¹⁵Icahn School of Medicine at Mount Sinai, The Charles Bronfman Institute for Personalized Medicine, New York, NY, USA, ¹⁶Department of Medicine, Division of Genetic Medicine, Vanderbilt University, Nashville, TN, USA, ¹⁷Zilber School of Public Health, University of Wisconsin-Milwaukee, Milwaukee, WI, USA, ¹⁸Département de Pharmacologie et Physiologie, Faculty of Medicine, Université de Montréal, Montreal, Quebec, Canada, ¹⁹Center for Genetic Epidemiology, Department of Preventive Medicine, Keck School of Medicine, University of Southern California, Los Angeles, CA,

USA, ²⁰Department of Statistics and Operation Research, University of North Carolina, Chapel Hill, NC, USA, ²¹Department of Ocular Pathology and Imaging Science, Graduate School of Medical Sciences, Kyushu University, Fukuoka, Japan, ²²Department of Biostatistics, University of Washington, Seattle, WA, USA, ²³Population Health Sciences, Bristol Medical School, University of Bristol, Bristol, UK, ²⁴Translational Health Sciences, Musculoskeletal Research Unit, Bristol Medical School, University of Bristol, Bristol, UK, ²⁵Novo Nordisk Foundation Center for Basic Metabolic Research, Faculty of Health and Medical Sciences, University of Copenhagen, Copenhagen, Denmark, ²⁶Hasso-Plattner-Institut, Universität Potsdam, Postdam, Germany, ²⁷Department of Medicine, University of Washington, Seattle, WA, USA, ²⁸Department of Epidemiology, Erasmus University Medical Center Rotterdam, Rotterdam, The Netherlands, ²⁹Laboratory of Epidemiology and Population Science, National Institute on Aging/NIH, Baltimore, MD, USA, ³⁰Massachusetts Veterans Epidemiology Research and Information Center (MAVERIC), VA Boston Healthcare System, Boston, MA, USA, ³¹Department of Medicine, Division on Aging, Brigham and Women's Hospital, Boston, MA, USA, ³²Department of Medicine, Harvard Medical School, Boston, MA, USA, ³³Division of Research, Kaiser Permanente Northern California, Oakland, CA, USA, ³⁴Department of Medicine, University of Mississippi Medical Center, Jackson, MS, USA, ³⁵Health Data Research UK Cambridge, Wellcome Genome Campus and University of Cambridge, Cambridge, UK, ³⁶The National Institute for Health Research Blood and Transplant Unit (NIHR BTRU) in Donor Health and Genomics at the University of Cambridge, Cambridge, UK, ³⁷Human Genetics, Wellcome Sanger Institute, Saffron Walden, UK, ³⁸National Institute for Health Research Cambridge Biomedical Research Centre, Cambridge University Hospitals, Cambridge, UK, ³⁹British Heart Foundation Centre of Excellence, Division of Cardiovascular Medicine, Addenbrooke's Hospital, Cambridge, UK, ⁴⁰Section of Nutrition and Metabolism, International Agency for Research on Cancer, Lyon, France, ⁴¹Department of Hygiene and Epidemiology, University of Ioannina Medical School, Ioannina, Greece, ⁴²Department of Internal Medicine, Section of Gerontology and Geriatric Medicine, Wake Forest School of Medicine, Winston-Salem, NC, USA, ⁴³Department of Epidemiology and Biostatistics, Imperial College London, London, UK, ⁴⁴Imperial Biomedical Research Centre, Imperial College London and Imperial College NHS Healthcare Trust, London, UK, ⁴⁵Medical Research Council-Public Health England Centre for Environment, Imperial College London, London, UK, ⁴⁶UK Dementia Research Institute, Imperial College London, London, UK, ⁴⁷Health Data research UK-London, London, UK, ⁴⁸Department of Epidemiology, University of Washington, Seattle, WA, USA, ⁴⁹Department of Internal Medicine, Erasmus University Medical Center Rotterdam, Rotterdam, The Netherlands, ⁵⁰Department of Neurology, University of Pennsylvania, Philadelphia, PA, USA, ⁵¹Institute for Immunology and Transfusion Medicine, University Medicine Greifswald, Greifswald, Germany, ⁵²Division of Public Health Sciences, Fred Hutchinson Cancer Research Center, Seattle, WA, USA, ⁵³Department of Genetics, Shanghai-MOST Key Laboratory of Health and Disease Genomics, Chinese National Human Genome Center and Shanghai Industrial Technology Institute (SITI), Shanghai, China, ⁵⁴Interfaculty Institute of Genetics and Functional Genomics, University Medicine Greifswald, Greifswald, Germany, ⁵⁵Chair of Experimental Bioinformatics, Research Group Computational Systems Medicine, Technical University of Munich, Freising-Weihenstephan, Germany, ⁵⁶German Center for Cardiovascular Research (DZHK), Partner Site Greifswald, Greifswald, Germany, ⁵⁷Department of Clinical Physiology, Tampere University Hospital, Tampere, Finland, ⁵⁸Department of Clinical Physiology, Finnish Cardiovascular Research Center - Tampere, Faculty of Medicine and Health Technology, Tampere University, Tampere, Finland, ⁵⁹Laboratory of Complex Trait Genomics, Department of Computational Biology and Medical Sciences, Graduate School of Frontier Sciences, The University of Tokyo, Tokyo, Japan, ⁶⁰Analytic and Translational Genetics Unit, Massachusetts General Hospital, Boston,

MA, USA, ⁶¹Department of Medicine, University of Colorado Denver, Anschutz Medical Campus, Aurora, CO, USA, ⁶²Department of Clinical Chemistry, Fimlab Laboratories, Tampere, Finland, ⁶³Department of Clinical Chemistry, Finnish Cardiovascular Research Center - Tampere, Faculty of Medicine and Health Technology, Tampere University, Tampere, Finland, ⁶⁴Department of Internal Medicine, University Medicine Greifswald, Greifswald, Germany, ⁶⁵Center for Clinical Research and Prevention, Bispebjerg and Frederiksberg Hospital, Frederiksberg, Denmark, ⁶⁶Department of Clinical Medicine, Faculty of Health and Medical Sciences, University of Copenhagen, Copenhagen, Denmark, ⁶⁷Department of Medicine, Division of Cardiology, Duke Molecular Physiology Institute, Duke University Medical Center, Durham, NC, USA, ⁶⁸Center for Public Health Genomics, University of Virginia, Charlottesville, VA, USA, ⁶⁹Department of Computational Biology and Medical Sciences, Graduate school of Frontier Sciences, The University of Tokyo, Tokyo, Japan, ⁷⁰Division of Molecular Pathology, the Institute of Medical Sciences, The University of Tokyo, Tokyo, Japan, ⁷¹Institute of Clinical Chemistry and Laboratory Medicine, University Medicine Greifswald, Greifswald, Germany, ⁷²Department of Cardiology, Heart Center, Tampere University Hospital, Tampere, Finland, ⁷³Department of Cardiology, Finnish Cardiovascular Research Center - Tampere, Faculty of Medicine and Health Technology, Tampere University, Tampere, Finland, ⁷⁴Department of Hematology, University of Cambridge, Cambridge Biomedical Campus, Cambridge, UK, ⁷⁵National Health Service (NHS) Blood and Transplant, Cambridge Biomedical Campus, Cambridge, UK, ⁷⁶Department of Laboratory Medicine and Pathology, University of Minnesota, Minneapolis, MN, USA, ⁷⁷Departments of Epidemiology, University of Washington, Seattle, WA, USA, ⁷⁸Department of Health Services, University of Washington, Seattle, WA, USA, ⁷⁹Kaiser Permanente Washington Health Research Institute, Seattle, WA, USA, ⁸⁰Centre for Population Health Research, University of Turku and Turku University Hospital, Turku, Finland, ⁸¹Research Centre of Applied and Preventive Cardiovascular Medicine, University of Turku, Turku, Finland, ⁸²Department of Clinical Physiology and Nuclear Medicine, Turku University Hospital, Turku, Finland, ⁸³Radcliffe Department of Medicine, University of Oxford, John Radcliffe Hospital, Oxford, UK, ⁸⁴Department of Haematology, Churchill Hospital, Oxford, UK, ⁸⁵Department of Biostatistics, University of North Carolina, Chapel Hill, NC, USA, ⁸⁶The Institute for Translational Genomics and Population Sciences, Department of Pediatrics, The Lundquist Institute for Biomedical Innovation (formerly Los Angeles Biomedical Research Institute) at Harbor-UCLA Medical Center, Torrance, CA, USA, ⁸⁷Department of Genetics, Stanford University School of Medicine, Stanford, CA, USA, ⁸⁸Department of Medicine, Faculty of Medicine, Université de Montréal, Montreal, Quebec, Canada, ⁸⁹Institute for Community Medicine, University Medicine Greifswald, Greifswald, Germany, ⁹⁰Atlanta VA Medical Center, Decatur, GA, USA, ⁹¹Department of Computer Science, University of North Carolina, Chapel Hill, NC, USA, ⁹²Quantitative and Computational Biology Section, Department of Biological Sciences, University of Southern California, Los Angeles, CA, USA, ⁹³Department of Molecular Physiology and Biophysics, Vanderbilt University, Nashville, TN, USA, ⁹⁴National Health Service Blood and Transplant, Cambridge, UK, ⁹⁵Laboratory of Statistical Immunology, Osaka University Graduate School of Medicine, Suita, Osaka, Japan.

*These authors contributed equally to this work.

†A list of members and their affiliations appears in the **Supplementary Information**.

§These authors jointly supervised this work.

Correspondence to:

Paul L. Auer

Joseph J. Zilber School of Public Health
KIRC 5067
PO Box 413
Milwaukee, WI, 53205-2557
414-229-2986
pauer@uwm.edu

Guillaume Lettre

Montreal Heart Institute
5000 Belanger St
Montreal, Quebec, Canada
H1T 1C8
514-376-3330 ext. 2657
guillaume.lettre@umontreal.ca